Mapping Asian anthropogenic emissions of non-methane volatile organic compounds to multiple chemical mechanisms

M. Li[1,2], Q. Zhang[1], D. G. Streets[3], K. B. He[2], Y. F. Cheng[4], L. K. Emmons[5], H. Huo[6], S. C. Kang[2], Z. Lu[3], M. Shao[7], H. Su[4], X. Yu[8], and Y. Zhang[9]

[1]{Ministry of Education Key Laboratory for Earth System Modeling, Center for Earth System Science, Tsinghua University, Beijing, China}

[2]{State Key Joint Laboratory of Environment Simulation and Pollution Control, School of Environment, Tsinghua University, Beijing, China}

[3]{Decision and Information Sciences Division, Argonne National Laboratory, Argonne, IL, USA}

[4]{Multiphase Chemistry Department, Max Planck Institute for Chemistry, Mainz, Germany}

[5]{Atmospheric Chemistry Division, National Center for Atmospheric Research, Boulder, CO, USA}

[6]{Institute of Energy, Environment and Economy, Tsinghua University, Beijing, China}

[7]{State Key Joint Laboratory of Environmental Simulation and Pollution Control, College of Environmental Sciences and Engineering, Peking University, Beijing, China}

[8]{Beijing Green Resource Research Co. Ltd., Beijing, China}

[9]{Department of Marine, Earth and Atmospheric Sciences, North Carolina State University, Raleigh, North Carolina, USA}

Correspondence to: Q. Zhang (qiangzhang@tsinghua.edu.cn)

Abstract

An accurate speciation mapping of non-methane volatile organic compounds (NMVOC) emissions has an important impact on the performance of chemical transport models (CTMs) in simulating ozone mixing ratios and secondary organic aerosols. Taking the INTEX-B Asian NMVOC emission inventory as the case, we developed an improved speciation framework to generate model-ready anthropogenic NMVOC emissions for various gas-phase chemical mechanisms commonly used in CTMs in this work, by using an explicit assignment approach and updated NMVOC profiles. NMVOC profiles were selected and aggregated from a wide range of new measurements and the SPECIATE database v4.2. To reduce potential uncertainty from individual measurements, composite profiles were developed by grouping and averaging source profiles from the same category. The fractions of oxygenated volatile organic compounds (OVOC) were corrected during the compositing process for those profiles which used improper sampling and analyzing methods. Emissions of individual species were then lumped into species in different chemical mechanisms used in CTMs by applying mechanism-dependent species mapping tables, which overcomes the weakness of inaccurate mapping in previous studies. Emission estimates for individual NMVOC species differ between one and three orders of magnitude for some species when different sets of profiles are used, indicating that source profile is the most important source of uncertainties of individual species emissions. However, those differences are diminished in lumped species as a result of the lumping in the chemical mechanisms. Gridded emissions for eight chemical mechanisms at 30 min $\times$ 30 min resolution as well as the auxiliary data are available at: http://mic.greenresource.cn/intex-b2006. The framework proposed in this work can be also used to develop speciated NMVOC emissions for other regions.

1. Introduction

Non-methane volatile organic compounds (NMVOCs) include a variety of chemical species that can be emitted from biomass burning, biogenic, and anthropogenic sources (Guenther et al., 2012; Piccot et al., 1992; van der Werf et al., 2010). NMVOCs are of great concern because they play a key role in tropospheric chemistry as precursors of ozone and secondary organic aerosols (SOA) and many NMVOC species do damage to human health. NMVOCs differ significantly in their impacts on ozone and SOA formation, and these differences need to be represented appropriately in chemical transport models (CTMs). Such CTMs have been used to guide the development of emission control strategies by governmental agencies (e.g., US EPA, 2007; Wang et al., 2010; Xing et al., 2011), predict the effects of changes of emissions on the formation of ozone and SOA (e.g., Hogrefe et al., 2004; Y. Zhang et al., 2010, 2013), and study the sensitivity of the model predictions of pollutant concentrations to different gas-phase chemical mechanisms (e.g., Kim et al., 2011; Zhang et al., 2012).

In CTMs, atmospheric chemical reactions are usually characterized by a specific chemical mechanism, in which many individual NMVOC species are lumped together according to similarities in chemical structure or reactivity. The most commonly used chemical mechanisms in CTMs include: the State Air Pollution Research Center 1999 version (SAPRC-99, Carter, 2000) and an updated version SAPRC-07 (Carter, 2010); Carbon Bond Mechanism version IV (CB-IV, Grey et al., 1989) and two variants with updates in reactions and related kinetic data including the Carbon Bond Mechanism version Z (CBMZ, Zaveri and Peters, 1999) and CB05 (Yarwood et al., 2005); as well as the second generation Regional Acid Deposition Model chemical mechanism (RADM2, Stockwell et al., 1990) and its variants with updates in reactions and related kinetic data including the Regional Atmospheric Chemistry Mechanism (RACM, Stockwell et al., 1997) and RACM2 (Goliff et al., 2013). This has been a challenge to map speciated NMVOC emissions data with organic compounds treated in different

chemical mechanisms through a translation scheme from total NMVOC emissions to lumped, model-ready emissions. In the US National Emission Inventory system, The Sparse Matrix Operator Kernel Emissions (SMOKE) modeling system has been developed with the function of preparing model-ready NMVOC emissions as inputs for any chemical mechanisms (e.g., CB05, SAPRC-99, RADM2) used in CTMs. In the SMOKE model, total NMVOC emissions are first split into individual species by assigning appropriate source profiles from the US EPA's SPECIATE database (Hsu and Divita, 2009; Simon et al., 2010) using source classification codes, and then aggregated to lumped model species treated in different chemical mechanisms using corresponding mechanism-dependent mapping tables (Houyoux et al., 2000).

For the Asian region, although speciated NMVOC emissions have been estimated by various regional and global inventories (e.g., Klimont et al., 2002; Streets et al., 2003; Ohara et al, 2007; Bo et al., 2008; Wei et al., 2008), the interfaces between NMVOC emissions and CTMs remain underdeveloped. Table 1 summarizes the existing global and regional NMVOC emission inventories covering Asia. In addition to the known uncertainties in estimates for the total NMVOC emission budget, there are two other major weaknesses in Asian emission inventory datasets. First, most inventory datasets are not ready for model input. Although many global and regional inventories provide emissions of chemical species groups for Asia, based on reactivity and structure similarity (see Table 1), those species groups differ from lumped model species used in chemical mechanisms. The mapping process between species in inventories and models was usually performed by modelers without a standard procedure, which may lead to inaccuracies and introduce unpredictable uncertainties. This is especially true for a lumped-structure mechanism (e.g., carbon bond mechanism) where organics are grouped by chemical bond type (Fu et al., 2009). Second, recent local measurements on NMVOC source profiles have not been updated in most inventory studies. It is believed that NMVOC source profiles vary among regions worldwide as the consequence of differences in fuel quality and combustion conditions.

111 For example, NMVOC composition from vehicles in China has been shown to be

112 significantly different from those in the US (Liu et al., 2008a). Recognizing this

113 problem, there are increasing numbers of measurements for local NMVOC source

114 profiles in Asia. They cover many of the most important sources, such as residential

115 fuel combustion (Tsai et al., 2003; Liu et al., 2008a; Wang et al., 2009), solvent use (Liu

116 et al., 2008a; Yuan et al., 2010), petrochemical industry (Liu et al., 2008a), on-road

117 transportation (Liu et al., 2008a; Lai et al., 2009), and fuel evaporation (Y. L. Zhang et

118 al., 2013). However, only some of these locally measured profiles have been used in

119 recent NMVOC emission inventories that covered part of China (Zheng et al., 2009) or

120 the transportation sector in China (Cai and Xie, 2007). An updated Asian NMVOC

121 emission database with state-of-the-art profiles is still missing.

122   In support of the US NASA Intercontinental Chemical Transport

123 Experiment-Phase B (INTEX-B) mission, we developed an air pollutant emission

124 inventory for Asia for the year 2006 (Zhang et al., 2009), including speciated

125 NMVOC emissions as model-ready inputs for various chemical mechanisms (i.e.,

126 SAPRC-99, SAPRC-07, CB-IV, CB05, and RADM2), processed by an explicit

127 speciation assignment approach. In the INTEX-B inventory, emissions for individual

128 VOC species are first calculated for each source category by applying profiles from

129 local measurements and the SPECIATE database, and individual species were lumped

130 to emitted species in different chemical mechanisms by corresponding species

131 mapping tables. The emissions dataset for the SAPRC-99 mechanism is available to

132 the public from http://mic.greenresource.cn/intex-b2006 and has been widely used in

133 CTMs (e.g., Wang et al., 2011; Lin et al., 2012; Dong et al., 2013).

134   Although the step-by-step speciation process used in the INTEX-B inventory has

135 provided model-ready NMVOC emission data to the community and reduced the

136 uncertainties associated with inaccurate speciation mapping procedure, there remain

137 many unresolved issues. Two major weaknesses are associated with profile selection

138 and processing and need to be addressed. First, the INTEX-B profiles omit some

139 important species, particularly oxygenated volatile organic compounds (OVOCs).

140 OVOCs, which include alcohols, aldehydes, ketones and ethers, play a key role in

141 atmospheric organic chemistry and many of them are known to have a detrimental

142 effect on human health (Christian et al., 2004; Fu et al., 2008; Hopkins et al., 2003).

143 The magnitude of OVOCs is significant and cannot be neglected for OVOC-rich

144 emitting sources, such as biofuel burning and diesel vehicle exhaust (Andreae and

145 Merlet, 2001; Schauer et al., 1999, 2001). Second, a single profile is assigned to each

146 specific source, which may introduce inaccuracy into the speciation process due to the

147 limitation of profiles (Cai and Xie, 2007; Reff et al., 2009). One limitation is that for

148 sources containing multiple fuels and technologies, such as biofuel combustion, a

149 single profile cannot represent the overall emission characteristics. On the other hand,

150 the quality of profiles is difficult to quantify and may introduce unpredictable levels

151 of uncertainty during profile selection.

152 In order to narrow the uncertainty from profile selection and processing

153 mentioned above, we followed the speciation framework of the INTEX-B inventory

154 but with necessary profile adjustments for OVOC-rich sources and the development

155 of composite profiles in this work. We also evaluated the impact of profile update on

156 the speciated emissions and ozone production, which is useful in understanding the

157 uncertainties in emission speciation and determining the source of discrepancies

158 between "bottom-up" emission inventories and "top-down" constraints (e.g., from

159 in-situ measurements and satellite observations).

160 This paper is organized as follows. Sect. 2 summarizes the methods and data that

161 were used in this work and the INTEX-B inventory, including total NMVOC

162 emissions, profile development, ozone formation potentials (OFPs) calculation,

163 mechanism species mapping, and spatial allocation. Sect. 3 presents and compares the

164 emissions of individual species and lumped mechanism species estimated in this work

165 and the original INTEX-B inventory. In Sect. 4, the sensitivity of emissions and OFPs

166 to profile selection is analyzed and the effects of updated profiles are assessed by

167 comparing OFPs calculated from the two estimates. Prospectives for future work are

168 discussed in Sect. 5.

169

170 **2. Methodology and data**

171   The general approach of speciation is to multiply total NMVOC emissions by a

172 corresponding chemical speciation profile for each source type. Figure 1 presents the

173 flow diagram of the methodology used in this work, as applied to the INTEX-B

174 inventory. In this work, we start from total NMVOC emission estimates for 2006 in

175 the INTEX-B Asian inventory (Zhang et al., 2009), select and aggregate profiles from

176 both local measurements and the SPECIATE database v.4.2 (Hsu and Divita, 2009),

177 and apply them to split total NMVOC into individual species. Compared to the

178 INTEX-B inventory, the main difference of this work is the use of composite profiles.

179 OFPs are calculated to evaluate the effect of profile update on ozone formation based

180 on the speciated NMVOC emissions developed in this work. Individual species are

181 lumped into model species of different mechanisms by specific mapping tables.

182 Finally, gridded emissions are developed at 30 min $\times$ 30 min resolution using various

183 spatial proxies.

184 **2.1 NMVOC emissions in 2006 for Asia**

185   Total NMVOC emissions were obtained from the 2006 Asian emission inventory

186 for the NASA INTEX-B mission (Zhang et al., 2009). This inventory is an update of

187 the TRACE-P Asian NMVOC inventory developed for an earlier NASA mission

188 (Streets et al., 2003) with significant improvement for China using detailed activity

189 data and local emission factors. The improved methodology for China led to a higher

190 degree of source specificity in China than other Asian countries. To compile a

191 speciated NMVOC emission dataset with consistent and comparable methodology for

192 all of Asia, a set of 55 source categories was aggregated by grouping similar source

193 types for China and other Asian regions. Anthropogenic NMVOC emissions for 2006

194   for each source category are tabulated in Table S1. As estimated in the INTEX-B

195   inventory, emissions from China (23.2 Tg) dominate total emissions in Asia (42% of

196   total), followed by Southeast Asia (14.1 Tg, 26%) and India (10.8 Tg, 20%).

197   Figure 2 presents the NMVOC emissions by eight sectors for China, Other regions

198   of East Asia, India, Other regions of South Asia and Southeast Asia. For all of Asia,

199   residential combustion, on-road transportation and industrial non-combustion

200   contribute most to the total emissions, whereas the sector distributions vary

201   significantly for different regions. For China, these three sectors share equally,

202   whereas industrial non-combustion dominates the emissions for Other East Asia. The

203   shares of residential combustion and on-road transportation are significant both for

204   India and Other South Asia. For Southeast Asia, the emissions of total NMVOC are

205   dominated by residential combustion and on-road transportation.

206   **2.2 Development and assignment of source profiles**

207   After classifying the INTEX-B total NMVOC emissions into grouped source

208   categories, the next step is to assign or create a profile for each source. For a given

209   source category, the profile development and assignment involve three steps: (1)

210   search candidate profiles, both from the SPECIATE database v.4.2 and local

211   measurements; (2) revise profiles that do not contain an OVOC contribution for

212   OVOC-rich sources; and (3) construct "composite" profile if more than one profile is

213   available.

214   The profiles are selected with the following steps. We first searched candidate

215   profiles from SPECIATE database v.4.2 and a variety of literatures for each source

216   category. The SPECIATE v4.2 database provides the most comprehensive collection

217   of available NMVOC profiles, containing more than 1600 source profiles from

218   measurements mainly in the US (Simon et al., 2010). Because the fuel quality,

219   combustion technology and emission regulations in Asia often differ significantly

220   from those in the US, profiles taken from the SPECIATE database may not represent

221 the chemical characteristics of sources accurately (Zheng et al., 2009). To develop a

222 database of state-of-the-art profiles for Asia, local profiles for each emitting source

223 type were gathered from the literature where available. As the numbers of

224 local-measured profiles are still very limited, we include all available "local" profiles

225 from literatures as candidate profiles. For those sources which local profiles are

226 available and we believe that there are significant differences between Asian and

227 western countries due to different technologies and/or legislations, only local profiles

228 are used (e.g. solvent use). For sources which similar technologies are used in Asian

229 and western countries (e.g., boilers, vehicles), profiles from SPECIATE database are

230 also included. In order to reduce the uncertainties associated with profile selection in

231 the original INTEX-B speciation process, as mentioned in Sect. 1, we take steps 2 and

232 3 respectively to solve the "OVOC" and "single profile" issue. We identified the

233 OVOC rich sources and corrected the incomplete profiles which missed OVOC

234 fraction. The "composite" profile for each source was finally developed with the same

235 weighting factor for each individual candidate profile. The specific procedure is

236 described below.

237 **2.2.1 Inclusion of OVOC in profiles**

238 From a comprehensive review of available profiles, we found that OVOCs

239 contribute a large fraction of total NMVOC emissions from biofuel combustion and

240 diesel vehicles (Schauer et al., 1999, 2001; Andreae and Merlet, 2001). However,

241 OVOC fractions are missing in some profiles for these two sources due to sampling

242 and analysis approaches (e.g., Liu et al., 2008a). Often, NMVOC samples were

243 collected by canisters and then analyzed by gas chromatographic (GC) techniques,

244 such as GC-mass spectrometry (GC-MS), GC-flame ionization detection (GC-FID),

245 and GC-electron capture detection (GC-ECD). These techniques have proved to be

246 accurate for determining the levels of hydrocarbons, but they are not suitable for

247 analyzing carbonyl species because they cannot quantify unstable and "sticky"

248 compounds accurately (Christian et al., 2004). Carbonyls are best analyzed by proton

9

249 transfer mass spectrometry (PTR-MS) online monitoring (Christian et al., 2004) or

250 collected by 2,4-dinitrophenylhydrazine (DNPH)-impregnated C18 cartridges and

251 then analyzed by high-performance liquid chromatography with UV detection

252 (HPLC/UV) (Schauer et al., 1999, 2001; Huang et al., 2011).

253 Until now, a standard protocol for NMVOC sampling and analysis is still not well

254 developed. Many local-measured profiles used canisters to collect samples and GC

255 techniques to analyze NMVOC species (e.g., Tsai et al., 2003; Liu et al., 2008a). In

256 this work, we still include those profiles in the speciation process after correcting their

257 OVOC fractions, as local-measured profiles are believed to better represent the

258 real-world conditions. The general procedure of the revision is to append "OVOC" as

259 a component to the original profile along with their percentage contribution calculated

260 from profiles with OVOC measured for the same source. The fraction of each species

261 except "OVOC" in the revised profile is calculated as:

262
$$X_{revised}(i, j) = \frac{X_{ori}(i, j)}{\sum_{j} X_{ori}(i, j)} \times \left(1 - \overline{X_{ovoc}(i, j)}\right) \quad (1)$$

263 Where i is the emitting source; j is the NMVOC species; $X_{ori}(i, j)$ and $X_{revised}(i, j)$ are

264 the fractions of species j in the original and revised profiles of emission source i,

265 respectively; X_{ovoc} is the proportion of OVOC for each selected profile that has OVOC

266 measured for source i; and $\overline{X_{ovoc}}$ is the calculated mean of X_{ovoc}. The mass fraction of

267 unspeciated "OVOC" in the revised profile is labeled with "missing value", not

268 involved in the speciation process.

269 Figure 3 demonstrates inclusion of the missing OVOC fraction for the crop

270 residue combustion profile measured by Liu et al. (2008). The average OVOC

271 fraction, calculated as 28.9% according to the four profiles that include OVOC

272 (Andreae and Merlet, 2001; Wang et al., 2009; and Profile No. 4420 and No. 4421 in

273 SPECIATE v.4.2), is used to scale the original profile proportionally. Inclusion of

274 OVOC fraction for diesel vehicle profiles is illustrated in Fig. S1. The revised profiles,

275 along with other selected profiles, are then added to the profile database, ready for the

276   next step of the speciation process.

277   **2.2.2 Development of composite profiles**

278   A "composite" profile is created for sources where multiple candidate profiles are

279   available. For a given source category, species along with their mass fractions in each

280   candidate profile are grouped and averaged, excluding missing values. It should be

281   noted that the OVOC fractions in incomplete profiles are determined to be missing

282   values, not involved in the calculation of average value. We choose median instead of

283   mean as average to help mitigate possible large errors stemming from the presence of

284   outlier samples and measurements (Reff et al., 2009). After the grouping and

285   averaging process, the "composite" profile is scaled to 100% proportionally. The

286   grouping and averaging process can reduce the uncertainties the empirical selection of

287   profiles. However, it may introduce additional uncertainties from the assumption that

288   each candidate profile for the same source is weighting equally.

289   Here we take the development of a composite profile for biofuel combustion as

290   an example. Eleven profiles for crop residue and wood combustion were selected and

291   processed into a composite profile, as listed from P1 to P11 in Fig. 4. The top 30

292   species and their corresponding fractions are presented, accounting for 84% of the

293   total mass in the composite profile. As shown in Fig. 4, measurements of species

294   exhibit a large diversity among profiles. First, none of these species are contained in

295   all profiles. In spite of the fact that species such as ethene, benzene and propane are

296   included in most of the profiles, the fractions for some species are only included in

297   one or two profiles (e.g., phenanthrene, glyoxal, and acetone), which introduces large

298   uncertainties in the composite profile. Second, for specific species, fractions from

299   different profiles vary significantly, revealing the discrepancies caused by different

300   fuels and technologies of the emitting source and/or different samples and techniques

301   used in the profile measurements. Thus, using a single profile will generate

302   considerably different emissions for individual species, indicating the huge

303   uncertainty associated with profile selection and application. The profile development

304   method used in this work, by selecting and averaging multiple profiles, is an
305   important way to reduce this uncertainty.

306   A complete list of profiles used in this work is presented in Table S1. The
307   composited profiles developed in this work are available from the following website:
308   http://mic.greenresource.cn/intex-b2006. The individual profiles for diesel vehicles
309   and the composite profile are illustrated in Fig. S2 as another example. After the
310   profile-assignment speciation, region- and source-specific speciated NMVOC
311   emissions for around 700 individual species are processed in this work, comprising
312   the basic emission dataset for lumping into different chemical mechanisms and OFPs
313   analysis.

2.3 Calculation of OFPs

315   The ozone reactivities for various NMVOC species differ significantly, which can
316   be scaled by the Maximum Incremental Reactivity (MIR) (Carter, 1994). OFP has
317   been widely used in assessing the roles of NMVOC emissions in ozone formation and
318   guiding the development of cost-effective ozone control measures (e.g., Song et al.,
319   2007; Zheng et al., 2009), which can be estimated based on mass and MIR for each
320   species. OFPs for individual species are calculated by multiplying emissions by
321   corresponding MIR values:

322    $$OFP(i,j,k) = EVOC(i,k) \times X(i,j) \times MIR(j) \quad (2)$$

323   Where $OFP(i,j,k)$ is the ozone formation potential of species j in region k, emitted
324   from source i; $EVOC(i,k)$ is the emission of total NMVOC for source i in region k;
325    $X(i,j)$ is the fraction of species j from the profile for source i, which is taken from
326   the composite profiles developed in this work; $MIR(j)$ is the maximum incremental
327   reactivity scale for species j. OFPs by chemical groups and by sectors are calculated
328   by summing up OFP values by corresponding individual species, to evaluate the
329   ozone formation potentials of different chemical groups and sectors. It should be
330   noted that species with no MIR values were ignored during the calculation of OFPs.

2.4 Assignments for different chemical mechanisms

In atmospheric models, individual VOC emissions are usually assigned to "lumped" species in a simplified mechanism to balance the accuracy and computational efficiency, according to the similarities of their chemical reactivity. In this work, emission assignments for various chemical mechanisms are calculated by multiplying the emissions of individual species by species- and mechanism-specific conversion factors as follows:

$$EVOC(i,k,m) = \sum_{j=1}^{n}\left[\frac{EVOC(i,k)\times X(i,j)}{mol(j)}\times C(j,m)\right] \quad (3)$$

Where k is the region; m is species type in a mechanism; n represents the number of species emitted from source i. $EVOC$ is the total NMVOC emissions; $X_{i,j}$ is the mass fraction of species j to total NMVOC emissions for source i, which is obtained from the composite profiles; $mol(j)$ is the mole weight of species j; and $C_{j,m}$ is the conversion factor of species j for mechanism category m. In this work, the conversion factors were taken from the mechanism-dependent mapping tables developed by Carter (2013).

For some profiles, a fraction of total NMVOC is assigned as "unknown" or "undefined" species, which probably reflects the unidentified fraction arising from the limitation of the analysis technique (Schauer et al., 1999). In this work, we treated the "unknown" species as a single species during the composite profile development and then assigned emissions from "unknown" species mainly into ALK5, NROG, OLE1, ARO1, and ARO2 in the SAPRC-99 mechanism and PAR, UNR, OLE, TOL, XYL, and ALDX in CB05, according to Carter (2013). However, the "unknown" species is not included in the OFP calculation, as its maximum incremental reactivity is undefined.

357   Emissions for six chemical mechanisms are calculated in this work based on the

358   availability of mapping tables in Cater (2013): CB-IV, CB05, SAPRC-99, SAPRC-07,

359   RADM2 and RACM2. These mapping tables are available at

360   http://www.engr.ucr.edu/~carter/emitdb/. In these tables, each individual organic

361   compound is assigned with conversion factors to mechanism species according to its

362   carbon bond (for CBIV and CB05) and chemical group (for SAPRC-99, SAPRC-07,

363   RADM2, and RACM2), hence it provides a consistent way of species mapping for

364   different chemical mechanisms. To our knowledge, this is the most accurate chemical

365   mapping approach in the community, which has been used in processing US emission

366   inventories. We also calculated emissions for two global models, GEOS-Chem and

367   MOZART-4, by lumping SAPRC-99 species to emission species in those two global

368   models. The mapping tables from SAPRC-99 species to GEOS-Chem and MOZART-4

369   species are presented in Tables 2 and 3 and the abbreviations of those species are

370   provided in Tables A1-A4.

371   **2.5 Spatial allocation**

372   Emissions are gridded for CTMs and aggregated into four sectors (power, industry,

373   residential and transportation), both by individual species and by chemical

374   mechanisms. We followed the top-down approach used in the INTEX-B inventory

375   (Zhang et al., 2009) to distribute country- or provincial-level emissions to grids using

376   various spatial proxies at 1 km × 1 km resolution (Streets et al., 2003; Woo et al., 2003).

377   Spatial proxies used in this work include: total population data extracted from

378   LandScan Global Population Dataset developed by Oak Ridge National Laboratory

379   (ORNL, 2004), urban and rural population data developed from partitioning total

380   population using urban land cover from LandScan 2000 database (ORNL, 2002), and

381   road networks from the Digital Chart of the World (DCW, 1993).

382   Table 4 listed the spatial proxies used in this work. All power generation units

383   with capacity larger than 300MW in China are identified as large point sources, while

384   other plants are treated as area sources and distributed by total population. Urban

385   population was used for distributing emissions from industrial combustion, residential

386   coal-fired boilers; rural population was used for residential biofuel combustion and

387   off-road transportation; road networks were used for on-road transportation emissions;

388   and total population was used for all other area sources. The final gridded emissions

389   were aggregated to 30 min $\times$ 30 min resolution.

390   3. Results

391   3.1 Speciated NMVOC Emissions by individual species

392   Using the approaches described in Sect. 2, emissions of ~700 individual NMVOC

393   species for Asia are estimated for the year 2006. Figure 5 presents emissions of the 30

394   species with the highest OFPs for the whole Asian region. These top 30 species

395   contributed 44% to total Asian anthropogenic NMVOC emissions and 82% to total

396   OFPs. For species with small emissions, the emission estimates have high uncertainty

397   due to the inaccuracy of the emission profiles and omission of minor emitting source

398   types.

399   As shown in Fig. 5, the order of OFPs of the top 30 species differs significantly

400   from that of emissions (by mass), which is attributed to the variation of chemical

401   reactivity of species, scaled by MIR in this work. Emphasis is placed on OVOCs and

402   alkenes with high MIRs and relatively high contribution to OFPs. It is interesting to

403   notice that some OVOCs, such as glyoxal and methylglyoxal, are determined to have

404   high OFPs but relatively low emission estimates, due to their high reactivity scales.

405   Alkanes and some aromatics (e.g., benzene) tend to be less chemically reactive in the

406   atmosphere and have lower contribution to OFPs compared to their emissions.

407   Figure 5 also shows the distribution of individual species emissions among major

408   contributing source types (by fuel type and by sector). Gasoline and biofuel

409   combustion are two common significant contributing sources for most species, with

410   the exception of a high proportion of contribution from non-combustion sources for

15

aromatics (e.g., 34% for xylene, 54% for toluene). Ethene is the largest contributor to ozone formation potential (29.0 Tg-O_3) with the second highest emissions (3.2 Tg), coming mainly from biofuel combustion (1.2 Tg, 38% of total), gasoline combustion (1.0 Tg, 32%), coal combustion (0.3 Tg, 10%), and non-combustion sources (0.3 Tg, 10%). Alkenes other than ethene such as propene, 2-methyl-2-butene, 1-butene also have significant contributions to OFPs. Propene is the third largest contributor to ozone formation, having similar distribution by fuel and sector as ethene. Important aromatic ozone precursors include xylenes, toluene, and 1,2,4-trimethylbenzene. We estimate that xylene emissions in Asia in 2006 were 3.4 Tg (27.2 Tg-O_3 ozone formation potential), ranking first in terms of magnitude of emissions and second in terms of OFPs.

As shown in Fig. 5, glyoxal, formaldehyde, methylglyoxal, acetaldehyde, and ethyl alcohol are OVOC species with remarkable contributions to anthropogenic OFPs over Asia. Some of OVOCs (e.g., glyoxal and methylglyoxal) also have important contributions to SOA formation through aqueous-phase reactions in aerosols and clouds (Carlton et al., 2007; Ervens and Volkamer, 2010). In this work, primary glyoxal and methylglyoxal are mostly emitted from biofuel combustion. However, it should be noted that incomplete profiles for other sources resulting from inappropriate sampling and analysis methods are a potential source of high uncertainty; newly measured profiles may provide additional sources of these OVOC species in the future.

Figure 6 compares the emissions of individual species estimated in this work and the original INTEX-B emission inventory, based on the same total NMVOC emission estimates. A total of 425 species were presented in Fig. 6, covering the species with annual emissions larger than 10 Mg in two inventories. Large differences are observed, having a general pattern of more OVOC and alkenes emissions estimated from this work than in the original INTEX-B inventory. For 132 species (31% of total), the differences between the two estimates were within 100%, while emission estimates

439 for 60 species (14% of total) differ by one order of magnitude or more, implying that

440 large uncertainties are introduced from NMVOC source profiles. Considering that the

441 uncertainties associated with activity rates and total NMVOC emission factors are

442 usually less than 100% (Zhao et al., 2011), the source profiles could be recognized as

443 the most important source of uncertainties in emission estimates for individual

444 NMVOC species. This, in turn, has significant implications for the ability of CTMs to

445 reliably model the oxidizing nature of the Asian atmosphere.

446 Compared to the original INTEX-B inventory, this work estimated much lower

447 emissions for acetylene, but much higher emissions for xylene and glyoxal (as shown

448 in Fig. S3). The significant decrease of acetylene emissions and increase of xylene

449 and glyoxal emissions are mainly due to the change of residential biofuel combustion

450 profile. As can be seen from Fig. 4, the profile used in the original INTEX-B

451 inventory is taken from Tsai et al. (2003) (P2 and P8), which contains high mass

452 fraction of acetylene (27.4% for P2 and 27.0% for P8, respectively) in contrast to the

453 composite profile.

454 For species like ethene, benzene and acetylene, emissions are lower than in the

455 INTEX-B inventory; whereas propene, xylene, glyoxal, acetone, and methyl alcohol

456 emissions are higher. Because alkenes, aromatics and OVOC are reactive precursors

457 for ozone and SOA formation, these differences in emissions may lead to

458 enhancements in OFPs and ozone and SOA concentrations simulated by CTMs. The

459 impact of emission differences from the speciation process on OFPs will be quantified

460 and discussed in the next section.

461 Figure 7 shows the spatial distribution of toluene emissions in 2006 at 30 min $\times$

462 30 min horizontal resolution. Gridded emissions for ~700 individual species at the

463 same resolution are all developed following the methodologies described in Sect. 2.5

464 and are available by request. These datasets would be useful for comparing with

465 in-situ measurements and identifying possible sources of uncertainties in emission

466 inventories (e.g., Wang et al., 2013). However, as emissions of some species may

467 differ by 1-3 orders of magnitude when assigning different sets of profiles, these

468 datasets should be used with caution in interpreting the discrepancy between

469 observations and NMVOC emissions, because the discrepancy may be attributed to

470 uncertainties in the profiles rather than in total NMVOC emissions.

471 **3.2 Speciated NMVOC emissions by chemical groups**

472   Figures 8 and 9 present 2006 NMVOC emissions in Asia by chemical groups

473 estimated in this work. We estimate that alkenes accounted for the largest share of

474 Asian total NMVOC emissions in 2006 (240 Gmole (10^9 mole), 30% of total),

475 followed by alkanes (191 Gmole, 24%), OVOCs (155 Gmole, 17%), aromatics (114

476 Gmole, 14%), and alkynes (56 Gmole, 7%). The shares from alkanes and aromatics

477 are larger in Japan and South Korea (Other East Asia) than in other regions, reflecting

478 the significant contribution from the industrial sector in the two countries.

479   We also compared emissions estimated in this work with the original INTEX-B

480 inventory by chemical groups in Figs. 8 and 9. In contrast to the large differences in

481 emission estimates for individual species, the discrepancies are reduced greatly after

482 grouping individual species into similar chemical functional groups. The emission

483 differences of alkanes, alkenes, and aromatics are within 5% between the original

484 INTEX-B inventory and this work, while significant differences were still found for

485 alkynes and OVOC emissions. A large increase compared to the original INTEX-B

486 inventory is observed for OVOC emissions, from 53 Gmoleyr^{-1} to 155 Gmoleyr^{-1}, in

487 contrast to the decrease of alkynes emissions from 261 Gmoleyr^{-1} to 56 Gmoleyr^{-1}.

488 Similar differences are found in all Asian regions except Other East Asia, where the

489 two estimates show similar distributions among chemical groups.

490   The dramatic increase for OVOC emissions and decrease for alkynes emissions is

491 dominated by the residential sector, mainly due to the creation and application of the

492 "composite" profile for biofuel combustion. The P2 and P8 profiles (both measured by

493 Tsai et al., 2003) that were used in the original INTEX-B speciation process are

494 incomplete profiles that miss the contributions from OVOCs. The increase of OVOC

495 emissions is due to the inclusion of the OVOC fraction in the "composite" profile.

496 Compared to P2 and P8, other candidate profiles have a much lower contribution from

497 acetylene (see Fig. 4), leading to the lower share of alkynes in the "composite" profile

498 used in this work. The inclusion of OVOC in incomplete profiles further decreases the

499 contributions for non-OVOC species, which also contribute to the differences in

500 alkyne contributions.

3.3 Model-ready emissions

502   One of the key objectives of this study is to develop model-ready NMVOC

503 emission datasets for Asian anthropogenic sources as the emission inputs for CTMs.

504 In this work, model-ready emissions for eight chemical mechanisms were developed:

505 CB-IV, CB05, SAPRC-99, SAPRC-07, RADM2, RACM2, GEOS-Chem, and

506 MOZART-4. Emissions for the GEOS-Chem model and MOZART-4 model were

507 converted from SAPRC-99 emissions using the species mapping tables presented in

508 Tables 2 and 3. Fig. 10 illustrates the 2006 Asian anthropogenic NMVOC emissions

509 lumped by SAPRC-99 and CB05 species. Emissions are then distributed by various

510 spatial proxies following the approaches described in Sect. 2.5 and aggregated at 30

511 min × 30 min resolution. Gridded emissions for the eight chemical mechanisms

512 mentioned   above   are   all   available   from   our   website

513 (http://mic.greenresource.cn/intex-b2006). Gridded emissions are provided for four

514 sectors: power plants, industry, residential, and transportation. Those data can be used

515 directly as model inputs without further species mapping. As an example, Fig. 11

516 presents the map of OLE1 (a SAPRC-99 species) emissions by sector covering all

517 regions included in this work, showing a broad spatial distribution among residential,

518 transportation and industry sectors.

519   As individual species are usually highly lumped in CTMs, it is important to

520 investigate how the speciation process impacts emissions in lumped species in

521 different mechanisms. In Fig. 10, we compare the speciated emissions assignments by

522 the SAPRC-99 and CB05 mechanisms, both in the INTEX-B inventory and this study.

523 The differences in lumped species emissions between the original INTEX-B inventory

524 and this work are much smaller compared to individual species, indicating that the

525 uncertainties associated with profile selection and processing are diminished as a

526 result of the lumping in the chemical mechanisms.

527   However, there are still significant differences between the two estimates. For

528 SAPRC-99 species, sharp increases of OVOC and ARO2 emissions from the

529 residential sector are found, contrasting with a decrease of ETHE (ethene) and ALK2

530 (primarily propane and acetylene) emissions for the same sector. OLE1 and OLE2

531 emissions from the transportation sector are larger in this work, contributing to the

532 differences in the two estimates for those two species. These differences are mainly

533 attributed to the updated profiles of biofuel combustion and on-road vehicles. The

534 differences between the two estimates by CB05 species show similar patterns as the

535 SAPRC-99 species (although this was represented in different lumping species), while

536 PAR emissions agree well between the two estimates, due to a high degree of

537 lumping.

538   Figure 12 further presents emissions by SAPRC-99 species for each Asian region

539 and compares with the original INTEX-B estimates. As the emission characteristics

540 for Other South Asia are very close to India, we present emissions of South Asia as a

541 whole. For South Asia and Southeast Asia, where emissions are dominated by the

542 residential sector, the two estimates differ significantly in OVOC, ALK2, and ETHE

543 emissions due to updates of profiles in residential and transportation sector, as

544 discussed above. For Other East Asia, the differences between the two estimates are

545 smaller, because the NMVOC emissions are dominated by the industrial sector in

546 which similar profiles were used.

547

4. Impacts of profile development on ozone production

4.1 Ozone Formation Potentials (OFPs)

548
549

550 Given the fact that emission estimates of individual NMVOC emissions in Asia
551 are heavily influenced by source profiles, it is important to understand how the
552 variations in emission estimates then impact the prediction of ozone production.
553 Based on the emissions by individual species and corresponding MIR, OFPs of Asian
554 anthropogenic NMVOC emissions in 2006 are calculated by sector and chemical
555 groups, as presented in Fig. 13.

556 The total OFPs of 2006 Asian anthropogenic NMVOC emissions calculated in this
557 work are 195 Tg-O_3, 33% higher than the OFPs from the original INTEX-B inventory,
558 indicating that the compilation of NMVOC source profiles can significantly impact
559 estimates of ozone production. In this work, we estimated that alkenes have the
560 largest contribution to total OFPs (46%), followed by aromatics (28%), OVOC (18%),
561 alkanes (7%), and alkynes (1%). Alkenes and OVOCs have larger contributions to
562 total OFPs than to total emissions, while alkanes and alkynes have smaller
563 contributions to OFPs due to their relatively low MIR.

564 Compared to the INTEX-B inventory, higher OFP contributions from alkenes,
565 aromatics, and OVCs are estimated. Higher OFPs from alkenes are mainly because
566 the locally measured profiles included for the transportation and industrial sectors
567 have higher proportions of propene and butenes, which have larger MIR than ethene.
568 Ethene contributes 34% to the total OFPs of alkenes in our new estimates, much
569 lower than the 58% in the original INTEX-B inventory. For aromatics, the emission
570 increase from aromatics other than benzene, especially xylenes with high ozone
571 reactivity, accounts for the increase of OFP. The increased in the OFP contribution
572 from OVOCs can be attributed to higher estimates of aldehyde emissions from the
573 residential sector. Note that total OFPs from the residential sector are almost the same
574 between the two estimates, which is mainly due an offsetting of the increase in

575   emissions of OVOC by a decrease in emissions of alkenes.

4.2 Sensitivity analysis of individual profiles

577   Since significant differences in emissions and OFPs are observed between the

578   original INTEX-B inventory and this work, which is attributed to the update of profile

579   selection and compilation, it is worth examining the sensitivity of individual profiles

580   to emission estimates and OFPs. From the analysis presented above, we found that the

581   profiles for biofuel combustion and on-road vehicles contributed significantly to those

582   differences. In this work, 11 biomass burning profiles covering different fuel types

583   and combustion conditions are used for compiling the "composite" profile of biofuel

584   combustion, as shown in Fig. 4. Emissions by individual species vary significantly

585   among these 11 profiles, which is partly due to the variation in fuel and combustion

586   types. When developing the Asian NMVOC emission inventory, such variations were

587   ignored by treating biofuel combustion as a single source category, due to the lack of

588   detailed statistics on fuel types and combustion conditions.

589   Based on the concept of MIR for individual species, we evaluate the ozone

590   reactivity scale for each profile by calculating OFPs per unit NMVOC emission, as

591   shown in Fig. 14, to determine the sensitivity of OFPs to source profiles. The profiles

592   from Andreae and Merlet (2001) (P1) and No. 4420 from the SPECIATE database

593   v.4.2 (P10) tend to produce more ozone when used in the speciation, because of the

594   high fractions of alkenes and OVOC, respectively. Since the OVOC fraction is

595   relatively high in P10, contributions to ozone formation from OVOC might be

596   overestimated if only P10 was used for biomass burning, whereas they may be

597   underestimated by using P2, P3, P6 or P7 (Tsai et al., 2003; Liu et al., 2008a), which

598   have no OVOC measured. The difference of OFP between the highest and the lowest

599   values from using different profiles is up to a factor of three, demonstrating the high

600   sensitivity of ozone formation to profiles. The composite profile represents the

601   average level of ozone formation for the biofuel combustion source.

22

602   We further compare the emissions of SAPRC-99 and CB05 species estimated with

603   those 11 different profiles and the composite profile, as presented in Fig. 15. It can be

604   seen that the standard deviations are very large for SAPRC-99, especially for ETHE

605   and ALK2, indicating that model simulations configured with SAPRC-99 mechanism

606   would be sensitive to profile selection. On the other hand, the variations in CB05

607   species are relatively small compared with SAPRC-99 species, which can be

608   explained by the high degree of lumping for CB05.

609   Sensitivity tests by both speciated emissions and ozone formation for diesel

610   vehicles are also performed, as showed in Fig. S4 and S5, drawing the same

611   conclusion that ozone formation potentials and model-ready emissions are very

612   sensitive to the profile selection and processing. The immediate implication is that

613   using a single profile will introduce large uncertainty into the speciation process, and

614   the composite profile developed in this work can combine the species information

615   from all profiles and represent the average emission characteristics of the emitting

616   source. Thus the uniform profile processing system that groups and aggregates

617   multiple profiles can reduce the uncertainty associated with profile selection,

618   especially when one-to-one mapping of emission source to profile is not feasible due

619   to the different degrees of source specificity.

620

621   **5. Discussion**

622   In this study, we developed a step-by-step assignment framework to map Asian

623   anthropogenic NMVOC emissions to eight chemical mechanisms used in different

624   CTMs. To our best knowledge, this is the first work providing model-ready NMVOC

625   emissions   database   over   Asia.   Compared   to   previous   work,   we   used

626   mechanism-specific mapping tables from Carter (2013) to accurately assign

627   individual NMVOC emissions to species groups in different chemical mechanisms,

628   which avoided the uncertainties from the species mapping process. We also compiled

629   "composite" profiles where more than one profile was available for a given source

630 category, to reduce the uncertainties arising from conflicting individual measurements
631 and the empirical selection of profiles.

632 Although we believe that the uncertainties in model-ready emissions provided by
633 this work are reduced significantly through our approach, they are still high, mainly
634 due to inadequacies in source profiles. More local measurements with standard
635 source-specific sampling and analysis methods are needed to reduce the discrepancies
636 among different measurements and enhance the data quality of profiles. Another
637 remaining uncertainty in this work is the mismatch between profile and source
638 classification in inventories. The level of detail in source profile measurements is
639 usually higher than that in the source categories of bottom-up inventories. The
640 composite profiles combined from different measurements then imply a hidden
641 assumption that each profile has the same weighting factor in that source category,
642 which is not always true. In future work, more detailed source category classification
643 that balances the complexity and data availability would help to narrow the
644 uncertainties.

645 Top-down constraints from in-situ observations provide useful information for
646 understanding emissions of NMVOC species through correlations between species
647 (e.g., Barletta et al., 2008; Tang et al., 2008) or source apportionment models (e.g.,
648 Liu et al., 2008a,b; Wang et al., 2013). Since profiles are key factors both in receptor
649 models (e.g., the chemical mass balance model) and speciated NMVOC inventory
650 developments, the inconsistency between "receptor-oriented" and "bottom-up"
651 emission estimates may be caused by differences in profile selection to some degree,
652 which needs more analysis in future work. Recent advancements in satellite
653 observations provide additional constraints on NMVOC emissions through
654 formaldehyde and glyoxal column densities (Wittrock et al., 2006; Fu et al., 2007; Liu
655 et al., 2012). Using glyoxal observations from the SCIAMACHY satellite instrument,
656 Liu et al. (2012) concluded that the underestimated aromatics emissions in current
657 inventories are the most likely missing source of glyoxal. From this work, we found

658   that primary emissions of glyoxal from biomass burning might be another important

659   source. Integration of bottom-up inventories and satellite observations would help to

660   close the gap between emission inventories and observations in the future.

661

662   **Acknowledgements**

668   Table A1. Description of SAPRC-99 NMVOC emitting species from anthropogenic
669   sources[a] .

Species in SAPRC-99	Description
ACET	Acetone
ALK1	Primarily ethane
ALK2	Primarily propane and acetylene
ALK3	Alkanes and other non-aromatic compounds that react only with OH, and have k_{OH} between 2.5×10^3 and 5×10^3 ppm^{-1} · min^{-1}
ALK4	Alkanes and other non-aromatic compounds that react only with OH, and have k_{OH} between 5×10^3 and 1×10^4 ppm^{-1} · min^{-1}
ALK5	Alkanes and other non-aromatic compounds that react only with OH, and have k_{OH} greater than 1×10^4 ppm^{-1} · min^{-1}
ARO1	Aromatics with $k_{OH} < 2 \times 10^4$ ppm^{-1} · min^{-1}
ARO2	Aromatics with $k_{OH} > 2 \times 10^4$ ppm^{-1} · min^{-1}
BACL	Biacetyl
BALD	Aromatic aldehydes (e.g., benzaldehyde)
CCHO	Methyl Hydroperoxide
CRES	Cresols
ETHE	Ethene
GLY	Glyoxal
HCHO	Formaldehyde
IPRD	Unsaturated aldehydes other than acrolein and methacrolein
MACR	Methacrolein
MEK	Ketones and other non-aldehyde oxygenated products which react with OH radicals slower than 5×10^{-12} cm^3 molec^{-2}·sec^{-1}
MEOH	Methyl alcohol
MGLY	Methylglyoxal
MVK	Aromatic aldehydes (e.g., benzaldehyde)
NROG	Unreactive organic chemicals
NVOL	Nonvolatile organic chemicals
OLE1	Alkenes (other than ethene) with $k_{OH} < 7 \times 10^4$ ppm^{-1} · min^{-1}
OLE2	Alkenes with $k_{OH} > 7 \times 10^4$ ppm^{-1} · min^{-1}
PHEN	Phenol
PRD2	Ketones and other non-aldehyde oxygenated products which react with OH radicals faster than 5×10^{-12} cm^3 molec^{-2}·sec^{-1}
RCHO	Lumped C3$^+$ Aldehydes

670   [a] Source: Carter (2000).

671

672 Table A2. Description of CB05 NMVOC emitting species from anthropogenic
673 sources[a] .

Species in CB05	Description
ALD2	Acetaldehyde
ALDX	Propionaldehyde and higher aldehydes
ETH	Ethene
ETHA	Ethane
ETOH	Ethyl alcohol
FORM	Formaldehyde
IOLE	Internal olefin carbon bond (R-C=C-R)
MEOH	Methyl alcohol
NVOL	Nonvolatile organic chemicals
OLE	Terminal olefin carbon bond (R-C=C)
PAR	Paraffin carbon bond (C-C)
TOL	Toluene and other monoalkyl aromatics
UNR	Unreactive VOCs
XYL	Xylene and other polyalkyl aromatics

674 [a] Source: http://www.camx.com/files/cb05_final_report_120805.aspx .

675

676 Table A3. Description of GEOS-CHEM NMVOC emitting species from
677 anthropogenic sources[a].

Species in GEOS-Chem	Description
ACET	Acetone
ALD2	Acetaldehyde
ALK4	Lumped >= C4 Alkanes
C2H6	Ethane
C3H8	Propane
CH2O	Formaldehyde
MEK	Methyl Ethyl Ketone
PRPE	Lumped >= C3 Alkenes

678 [a] Source: http://acmg.seas.harvard.edu/geos/doc/man/ .

679

680 Table A4. Description of MAZART-4 NMVOC emitting species from anthropogenic
681 sources[a] .

Species for MOZART-4	Description
BIGALK	Lumped alkanes C > 3
BIGENE	Lumped alkenes C > 3
TOLUENE	Lumped aromatics
C3H6	Propene
C3H8	Propane
C2H6	Ethane

C2H4	Ethene
MEK	Methyl ethyl ketone
CH2O	Formaldehyde
CH3CHO	Acetaldehyde
CH3COCH3	Acetone
CH3OH	Methyl alcohol
C2H5OH	Ethyl alcohol

682 [a] Source: Emmons et al. (2010).

683

684   **References**

685   Andreae, M. O., and Merlet, P.: Emission of trace gases and aerosols from biomass

686   burning, Glob. Biogeochem. Cy., 15, 955-966, doi: 10.1029/2000GB001382,

687   2001.

688   Barletta, B., Meinardi, S., Simpson, I. J., Zou, S., Sherwood Rowland, F., and Blake,

689   D. R.: Ambient mixing ratios of nonmethane hydrocarbons (NMHCs) in two

690   major urban centers of the Pearl River Delta (PRD) region: Guangzhou and

691   Dongguan, Atmos. Environ., 42, 4393-4408, 2008.

692   Bo, Y., Cai, H., and Xie, S. D.: Spatial and temporal variation of historical

693   anthropogenic NMVOCs emission inventories in China, Atmos. Chem. Phys., 8,

694   7297-7316, doi: 10.5194/acp-8-7297-2008, 2008.

695   Boeke, N. L., Marshall, J. D., Alvarez, S., Chance, K. V., Fried, A., Kurosu, T. P.,

696   Rappengluck, B., Richter, D., Walega, J., Weibring, P., and Millet, D. B.:

697   Formaldehyde columns from the Ozone Monitoring Instrument: Urban versus

698   background levels and evaluation using aircraft data and a global model, J.

699   Geophys. Res., 116, D05303, doi: 10.1029/2010JD014870, 2011.

700   Cai, H. and Xie, S.: Estimation of vehicular emission inventories in China from 1980

701   to 2005, Atmos. Environ., 41, 8963-8979, 2007.

702   Carlton, A. G., Turpin, B. J., Altieri, K. E., Seitzinger, S., Reff, A., Lim, H.-J., and

703   Ervens, B.: Atmospheric oxalic acid and SOA production from glyoxal: Results of

704   aqueous photooxidation experiments, Atmos. Environ., 41, 7588-7602, 2007.

705   Carter, W. P. L.: Development of ozone reactivity scales for volatile organic

706   compounds, J. Air Waste Manage., 44, 881-899, 1994.

707   Carter, W. P. L.: Documentation of the SAPRC-99 chemical mechanism for VOC

708   reactivity assessment, report to the California Air Resources Board, available at:

709   http://www.engr.ucr.edu/~carter/reactdat.htm (last access: October 2013), 2000.

710   Carter, W. P. L.: Development of the SAPRC-07 chemical mechanism, Atmos.

711   Environ., 44, 5324-5335, 2010.

712   Carter, W. P. L.: Development of an improved chemical speciation database for

713   processing emissions of volatile organic compounds for air quality models, report

714   available at: http://www.engr.ucr.edu/~carter/emitdb/ (last access: November

715   2013), 2013.

716   Christian, T. J., Kleiss, B., Yokelson, R. J., Holzinger, R., Crutzen, P. J., Hao, W. M.,

717   Shirai, T., and Blake, D. R.: Comprehensive laboratory measurements of

718   biomass-burning emissions: 2. First intercomparison of open-path FTIR, PTR-MS,

719   and GC-MS/FID/ECD, J. Geophys. Res., 109, D02311, doi:

720   10.1029/2003JD003874, 2004.

721   Dong, X., Gao, Y., Fu, J. S., Li, J., Huang, K., Zhuang, G., and Zhou, Y.: Probe into

722   gaseous pollution and assessment of air quality benefit under sector dependent

723   emission control strategies over megacities in Yangtze River Delta, China, Atmos.

724   Environ., 79, 841-852, 2013.

725   Duffy, B. L., Nelson, P. F., Ye, Y., and Weeks, I. A.: Speciated hydrocarbon profiles

726   and calculated reactivities of exhaust and evaporative emissions from 82 in-use

727   light-duty Australian vehicles, Atmos. Environ., 33, 291-307, 1999.

728   Duncan, B. N., Yoshida, Y., Olson, J. R., Sillman, S., Martin, R. V., Lamsal, L., Hu, Y.,

729   Pickering, K. E., Retscher, C., Allen, D. J., and Crawford, J. H.: Application of

730   OMI observations to a space-based indicator of NO_x and VOC controls on surface

731   ozone formation, Atmos. Environ., 44, 2213-2223, 2010.

732   Emmons, L. K., Walters, S., Hess, P. G., Lamarque, J. F., Pfister, G. G., Fillmore, D.,

733   Granier, C., Guenther, A., Kinnison, D., Laepple, T., Orlando, J., Tie, X., Tyndall,

734   G., Wiedinmyer, C., Baughcum, S. L., and Kloster, S.: Description and evaluation

735   of the Model for Ozone and Related chemical Tracers, version 4 (MOZART-4),

736   Geosci. Model Dev., 3, 43-67, doi: 10.5194/gmd-3-43-2010, 2010.

737   Ervens, B. and Volkamer, R.: Glyoxal processing by aerosol multiphase chemistry:

738   towards a kinetic modeling framework of secondary organic aerosol formation in

739   aqueous particles, Atmos. Chem. Phys., 10, 8219-8244, doi:

740 10.5194/acp-10-8219-2010, 2010.

741 Fu, J. S., Streets, D. G., Jang, C. J., Hao, J. M., He, K. B., Wang, L. T., and Zhang, Q.:

742 Modeling Regional/Urban Ozone and Particulate Matter in Beijing, China, J. Air

743 Waste Manage., 59, 37-44, 2009.

744 Fu, T. M., Jacob, D. J., Palmer, P. I., Chance, K., Wang, Y. X. X., Barletta, B., Blake,

745 D. R., Stanton, J. C., and Pilling, M. J.: Space-based formaldehyde measurements

746 as constraints on volatile organic compound emissions in east and south Asia and

747 implications for ozone, J. Geophys. Res., 112, D06312, doi:

748 10.1029/2006JD007853, 2007.

749 Fu, T.-M., Jacob D. J., Wittrock, F., Burrows, J. P., Vrekoussis, M., and Henze, D. K.:

750 Global budgets of atmospheric glyoxal and methylglyoxal, and implications for

751 formation of secondary organic aerosols, J. Geophys. Res., 113, D15303,

752 doi:10.1026/2007JD009505, 2008.

753 Gery, M. W., Whitten, G. Z., Killus, J. P., and Dodge, M. C.: A photochemical kinetics

754 mechanism for urban and regional scale computer modeling, J. Geophys. Res., 94,

755 12925–12956, 1989

756 Goliff, W. S., Stockwell, W. R., and Lawson, C. V.: The regional atmospheric

757 chemistry mechanism, version 2, Atmos. Environ., 68, 174–185, 2013.

758 Guenther, A. B., Jiang, X., Heald, C. L., Sakulyanontvittaya, T., Duhl, T., Emmons, L.

759 K., and Wang, X.: The Model of Emissions of Gases and Aerosols from Nature

760 version 2.1 (MEGAN2.1): an extended and updated framework for modeling

761 biogenic emissions, Geosci. Model Dev., 5, 1471-1492,

762 doi:10.5194/gmd-5-1471-2012, 2012.

763 Hogrefe, C., Lynn, B., Civerolo, K., Ku, J. Y., Rosenthal, J., Rosenzweig, C.,

764 Goldberg, R., Gaffin, S., Knowlton, K., and Kinney, P. L.: Simulating changes in

765 regional air pollution over the eastern United States due to changes in global and

766 regional climate and emissions, J. Geophys. Res., 109, D22301, doi:

767 10.1029/2004jd004690, 2004.

768 Hopkins, J. R., Lewis, A. C., and Read, K. A.: A two-column method for long-term
769   monitoring of non-methane hydrocarbons (NMHCs) and oxygenated volatile
770   organic compounds (o-VOCs), J. Environ. Monitor., 5, 8-13, doi:
771   10.1039/b202798d, 2003.

772 Houyoux, M. R., Vukovich, J. M., Coats, C. J., Wheeler, N. J. M., and Kasibhatla, P.
773   S.: Emission inventory development and processing for the Seasonal Model for
774   Regional Air Quality (SMRAQ) project, J. Geophys. Res., 105, 9079-9090, 2000.

775 Hsu, Y. and Divita, F.: SPECIATE 4.2, speciation database development
776   documentation, final report, EPA/600-R-09/-38, 2009.

777 Huang, Y., Ho, S. S. H., Ho, K. F., Lee, S. C., Yu, J. Z., and Louie, P. K. K.:
778   Characteristics and health impacts of VOCs and carbonyls associated with
779   residential cooking activities in Hong Kong, J. Hazard. Mater., 186, 344-351,
780   2011.

781 Kelly, T. J. and Holdren, M. W.: Applicability of canisters for sample storage in the
782   determination of hazardous air pollutants, Atmos. Environ., 29, 2595-2608, 1995.

783 Kim, Y., Couvidat, F., Sartelet, K., and Seigneur, C.: Comparison of different
784   gas-phase mechanisms and aerosol modules for simulating particulate matter
785   formation, J. Air Waste Manage., 61, 1218-1226, 2011.

786 Klimont, Z., Streets, D. G., Gupta, S., Cofala, J., Fu, L. X., and Ichikawa, Y.:
787   Anthropogenic emissions of non-methane volatile organic compounds in China,
788   Atmos. Environ., 36, 1309-1322, 2002.

789 Lai, C. H., Chang, C. C., Wang, C. H., Shao, M., Zhang, Y. H., and Wang, J. L.:
790   Emissions of liquefied petroleum gas (LPG) from motor vehicles, Atmos.
791   Environ., 43, 1456-1463, 2009.

792 Lamarque, J.-F., Bond, T. C., Eyring, V., Granier, C., Heil, A., Klimont, Z., Lee, D.,
793   Liousse, C., Mieville, A., Owen, B., Schultz, M. G., Shindell, D., Smith, S. J.,
794   Stehfest, E., Van Aardenne, J., Cooper, O. R., Kainuma, M., Mahowald, N.,
795   McConnell, J. R., Naik, V., Riahi, K., and van Vuuren, D. P.: Historical (1850–

796 2000) gridded anthropogenic and biomass burning emissions of reactive gases and

797 aerosols: methodology and application, Atmos. Chem. Phys., 10, 7017-7039,

798 doi:10.5194/acp-10-7017-2010, 2010.

799 Lin, M., Fiore, A. M., Horowitz, L. W., Cooper, O. R., Naik, V., Holloway, J., Johnson,

800 B. J., Middlebrook, A. M., Oltmans, S. J., Pollack, I. B., Ryerson, T. B., Warner, J.

801 X., Wiedinmyer, C., Wilson, J., and Wyman, B.: Transport of Asian ozone

802 pollution into surface air over the western United States in spring, J. Geophys.

803 Res., 117, D00V07, doi: 10.1029/2011JD016961, 2012.

804 Liu, Y., Shao, M., Fu, L. L., Lu, S. H., Zeng, L. M., and Tang, D. G.: Source profiles

805 of volatile organic compounds (VOCs) measured in China: Part I, Atmos.

806 Environ., 42, 6247-6260, 2008a.

807 Liu, Y., Shao, M., Lu, S., Chang, C.-C., Wang, J.-L., and Fu, L.: Source

808 apportionment of ambient volatile organic compounds in the Pearl River Delta,

809 China: Part II, Atmos. Environ., 42, 6261-6274, 2008b.

810 Liu, Z., Wang, Y., Vrekoussis, M., Richter, A., Wittrock, F., Burrows, J. P., Shao, M.,

811 Chang, C.-C., Liu, S.-C., Wang, H., and Chen, C.: Exploring the missing source of

812 glyoxal (CHOCHO) over China, Geophys. Res. Lett., 39, L10812, doi:

813 10.1029/2012GL051645, 2012.

814 Lu, H. X., Wen, S., Feng, Y. L., Wang, X. N., Bi, X. H., Sheng, G. Y., and Fu, J. M.:

815 Indoor and outdoor carbonyl compounds and BTEX in the hospitals of

816 Guangzhou, China, Sci. Total Environ., 368, 574-584, 2006.

817 Na, K., Kim, Y. P., Moon, I., and Moon, K. C.: Chemical composition of major VOC

818 emission sources in the Seoul atmosphere, Chemosphere, 55, 585-594, 2004.

819 Piccot, S. D., Watson, J. J., and Jones, J. W.: A global inventory of volatile organic

820 compound emissions from anthropogenic sources, J. Geophys. Res., 97,

821 9897-9912, 1992.

822 Reff, A., Bhave, P. V., Simon, H., Pace, T. G., Pouliot, G. A., Mobley, J. D., and

823 Houyoux, M.: Emissions Inventory of $PM_{2.5}$ Trace Elements across the United

824   States, Environ. Sci. Technol., 43, 5790-5796, 2009.

825 Schauer, J. J., Kleeman, M. J., Cass, G. R., and Simoneit, B. R. T.: Measurement of

826   emissions from air pollution sources. 2. C-1 through C-30 organic compounds

827   from medium duty diesel trucks, Environ. Sci. Technol., 33, 1578-1587, 1999.

828 Schauer, J. J., Kleeman, M. J., Cass, G. R., and Simoneit, B. R. T.: Measurement of

829   emissions from air pollution sources. 3. C-1-C-29 organic compounds from

830   fireplace combustion of wood, Environ. Sci. Technol., 35, 1716-1728, 2001.

831 Schauer, J. J., Kleeman, M. J., Cass, G. R., and Simoneit, B. R. T.: Measurement of

832   emissions from air pollution sources. 5. C-1-C-32 organic compounds from

833   gasoline-powered motor vehicles, Environ. Sci. Technol., 36, 1169-1180, 2002.

834 Simon, H., Beck, L., Bhave, P. V., Divita, F., Hsu, Y., Luecken, D., Mobley, J. D.,

835   Pouliot, G. A., Reff, A., Sarwar, G., and Strum, M.: The development and uses of

836   EPA's SPECIATE database, Atmos. Pollut. Res., 1, 196-206, 2010.

837 Song, Y., Shao, M., Liu, Y., Lu, S., Kuster, W., Goldan, P., and Xie, S.: Source

838   Apportionment of Ambient Volatile Organic Compounds in Beijing, Environ. Sci.

839   Technol., 41, 4348-4353, 2007.

840 Stockwell W. R., Middleton, P., Chang, J. S., and Tang, X.: The second generation

841   Regional Acid Deposition Model chemical mechanism for regional air quality

842   modeling, J. Geophys. Res., 95, 16343–16367, 1990.

843 Stockwell, W. R., Kirchner, F., Kuhn, M., and Seefeld, S.: A new mechanism for

844   regional atmospheric chemistry modeling, J. Geophys. Res., 102, 25847–25879,

845   1997.

846 Streets, D. G., Bond, T. C., Carmichael, G. R., Fernandes, S. D., Fu, Q., He, D.,

847   Klimont, Z., Nelson, S. M., Tsai, N. Y., Wang, M. Q., Woo, J. H., and Yarber, K. F.:

848   An inventory of gaseous and primary aerosol emissions in Asia in the year 2000, J.

849   Geophys. Res., 108, 8809, doi: 10.1029/2002JD003093, 2003.

850 Tang, J. H., Chan, L. Y., Chan, C. Y., Li, Y. S., Chang, C. C., Wang, X. M., Zou, S. C.,

851   Barletta, B., Blake, D. R., and Wu, D.: Implications of changing urban and rural

852   emissions on non-methane hydrocarbons in the Pearl River Delta region of China,

853   Atmos. Environ., 42, 3780-3794, 2008.

854   Tsai, S. M., Zhang, J. F., Smith, K. R., Ma, Y. Q., Rasmussen, R. A., and Khalil, M. A.

855   K.: Characterization of non-methane hydrocarbons emitted from various

856   cookstoves used in China, Environ. Sci. Technol., 37, 2869-2877, 2003.

857   US EPA: Guidance on the use of models and other analyses for demonstrating

858   attainment of air quality for ozone, $PM_{2.5}$ and regional haze, US Environmental

859   Protection Agency, United States, 253 pp., 2007.

860   van der Werf, G. R., Randerson, J. T., Giglio, L., Collatz, G. J., Mu, M., Kasibhatla, P.

861   S., Morton, D. C., DeFries, R. S., Jin, Y., and van Leeuwen, T. T.: Global fire

862   emissions and the contribution of deforestation, savanna, forest, agricultural, and

863   peat fires (1997-2009), Atmos. Chem. Phys., 10, 11707-11735, doi:

864   10.5194/acp-11707-2010, 2010.

865   Wang, L., Jang, C., Zhang, Y., Wang, K., Zhang, Q., Streets, D., Fu, J., Lei, Y.,

866   Schreifels, J., He, K., Hao, J., Lam, Y.-F., Lin, J., Meskhidze, N., Voorhees, S.,

867   Evarts, D., and Phillips, S.: Assessment of air quality benefits from national air

868   pollution control policies in China. Part II: Evaluation of air quality predictions and

869   air quality benefits assessment, Atmos. Environ., 44, 3449-3457, 2010.

870   Wang, M., Shao, M., Chen, W., Yuan, B., Lu, S., Zhang, Q., Zeng, L., and Wang, Q.:

871   Validation of emission inventories by measurements of ambient volatile organic

872   compounds in Beijing, China, Atmos. Chem. Phys. Discuss., 13, 26933-26979,

873   doi: 10.5194/acpd-13-26933-2013, 2013.

874   Wang, S., Wei, W., Du, L., Li, G., and Hao, J.: Characteristics of gaseous pollutants

875   from biofuel-stoves in rural China, Atmos. Environ., 43, 4148-4154, 2009.

876   Wang, X. M., Sheng, G. Y., Fu, J. M., Chan, C. Y., Lee, S. G., Chan, L. Y., and Wang,

877   Z. S.: Urban roadside aromatic hydrocarbons in three cities of the Pearl River

878   Delta, People's Republic of China, Atmos. Environ., 36, 5141-5148, 2002.

879   Wang, Y., Zhang, Y., Hao, J., and Luo, M.: Seasonal and spatial variability of surface

880   ozone over China: contributions from background and domestic pollution, Atmos.

881   Chem. Phys., 11, 3511-3525, 2011.

882   Wei, W., Wang, S. X., Chatani, S., Klimont, Z., Cofala, J., and Hao, J. M.: Emission

883   and speciation of non-methane volatile organic compounds from anthropogenic

884   sources in China, Atmos. Environ., 42, 4976-4988, 2008.

885   Wittrock, F., Richter, A., Oetjen, H., Burrows, J. P., Kanakidou, M., Myriokefalitakis,

886   S., Volkamer, R., Beirle, S., Platt, U., and Wagner, T.: Simultaneous global

887   observations of glyoxal and formaldehyde from space, Geophys. Res. Lett., 33,

888   L16804, doi: 10.1029/2006GL026310, 2006.

889   Woo, J. H., Baek, J. M., Kim, J. W., Carmichael, G. R., Thongboonchoo, N., Kim, S.

890   T., and An, J. H.: Development of a multi-resolution emission inventory and its

891   impact on sulfur distribution for Northeast Asia, Water Air Soil Poll., 148,

892   259-278, 2003.

893   Xing, J., Zhang, Y., Wang, S., Liu, X., Cheng, S., Zhang, Q., Chen, Y., Streets, D. G.,

894   Jang, C., Hao, J., and Wang, W.: Modeling study on the air quality impacts from

895   emission reductions and atypical meteorological conditions during the 2008

896   Beijing Olympics, Atmos. Environ., 45, 1786-1798, 2011.

897   Yarwood, G., Rao, S., Yocke, M., and Whitten, G.: Updates to the Carbon Bond

898   Chemical Mechanism: CB05, Final Report to the US EPA, RT-0400675, available

899   at: http://www.camx.com (last access: October 2013), 2005.

900   Yuan, B., Shao, M., Lu, S., and Wang, B.: Source profiles of volatile organic

901   compounds associated with solvent use in Beijing, China, Atmos. Environ., 44,

902   1919-1926, 2010.

903   Zaveri, R. A. and Peters, L. K.: A new lumped structure photochemical mechanism for

904   large-scale applications, J. Geophys. Res., 104, 30387–30415, doi:

905   10.1029/1999JD900876, 1999.

906   Zhang, Q., Streets, D. G., Carmichael, G. R., He, K. B., Huo, H., Kannari, A.,

907   Klimont, Z., Park, I. S., Reddy, S., Fu, J. S., Chen, D., Duan, L., Lei, Y., Wang, L.

908   T., and Yao, Z. L.: Asian emissions in 2006 for the NASA INTEX-B mission,

909   Atmos. Chem. Phys., 9, 5131-5153, doi: 10.5194/acp-9-5131-2009, 2009.

910   Zhang, Y., Liu, X.-H., Olsen, K. M., Wang, W.-X., Do, B. A., and Bridgers, G. M.:

911   Responses of future air quality to emission controls over North Carolina, Part II:

912   Analyses of future-year predictions and their policy implications, Atmos. Environ.,

913   44, 2767-2779, 2010.

914   Zhang, Y., Chen, Y., Sarwar, G., and Schere, K.: Impact of gas-phase mechanisms on

915   Weather Research Forecasting Model with Chemistry (WRF/Chem) predictions:

916   Mechanism implementation and comparative evaluation, J. Geophys. Res., 117,

917   D01301, doi: 10.1029/2011jd015775, 2012.

918   Zhang, Y., Wang, W., Wu, S.-Y., Kang, K., Minoura, H., and Wang, Z.-F.: Impacts of

919   updated emission inventories on source apportionment of fine particle and ozone

920   over the southeastern US, Atmos. Environ., under review, 2013.

921   Zhang, Y.L., Wang, X.M., Zhang, Z., Lu S.J., Shao, M., Lee, F.S.C., and Yu, J.Z.:

922   Species profiles and normalized reactivity of volatile organic compounds from

923   gasoline evaporation in China, Atmos. Environ., 79, 110-118, 2013.

924   Zhao, L. R., Wang, X. M., He, Q. S., Wang, H., Sheng, G. Y., Chan, L. Y., Fu, J. M.,

925   and Blake, D. R.: Exposure to hazardous volatile organic compounds, PM10 and

926   CO while walking along streets in urban Guangzhou, China, Atmos. Environ., 38,

927   6177-6184, 2004.

928   Zheng, J. Y., Shao, M., Che, W. W., Zhang, L. J., Zhong, L. J., Zhang, Y. H., and

929   Streets, D.: Speciated VOC Emission Inventory and Spatial Patterns of Ozone

930   Formation Potential in the Pearl River Delta, China, Environ. Sci. Technol., 43,

931   8580-8586, 2009.

932

Table 1. NMVOC emission inventories covering Asian regions

Inventory	Source[a]	Region	Year	Species included	Profiles used
EDGAR v2[b]	AN+BB	Global	1990	23 groups	Unknown
EDGAR v3[c] and v4[d]	AN+BB	Global	1970-2008	N/A	
POET[e]	AN+BB	Global	1990-2000	13 groups	Unknown
RETRO[f]	AN+BB	Global	1960-2000	22 groups	Unknown
Lamarque et al., 2010	AN+BB	Global	1850-2000	22 groups	From RETRO
Klimont et al., 2002	AN	China	1995	16 groups	SPECIATE
Streets et al., 2003	AN+BB	Asia	2000	19 groups	SPECIATE
Ohara et al., 2007[g]	AN+BB	Asia	1980-2003	N/A	
Kurokawa et al., 2013	AN+BB	Asia	2000-2008	19 groups	From Streets et al. (2003)
Bo et al., 2008	AN	China	1980-2005	N/A	
Wei et al., 2008	AN	China	2005	40 groups including major individual active species	Local profiles + SPECIATE
Zheng et al., 2009	AN+BG	PRD, China	2006	91 species from AN, and 30 species from BG	Local profiles + SPECIATE
Cai et al., 2009	Transportation	China	1980-2005	67 species	From literatures
This work	AN	Asia	2006	~700 individual species; then mapping to emitting species of 8 chemical mechanisms	

[a]AN = anthropogenic; BB = biomass burning; BG = biogenic.

[b]available at: http://www.pbl.nl/en/themasites/geia/emissions_data/nmvoc_groups/index.html.

[c]available at: http://themasites.pbl.nl/tridion/en/themasites/edgar/emission_data/edgar32/index-2.html.

[d]available at: http://edgar.jrc.ec.europa.eu/index.php; http://eccad.sedoo.fr.

[e]available at: http://www.aero.jussieu.fr/projet/ACCENT/POET.php; http://eccad.sedoo.fr.

[f]available at: http://retro.enes.org/data_emissions.shtml.

[g]not independent estimates. Data extrapolated from Klimont et al., 2002 and Streets et al., 2003.

Table 2. Mapping table from SAPRC-99 species to GEOS-Chem Species.

SAPRC-99	GEOS-Chem
ACET	ACET
CCHO	ALD2
ALK3+ALK4+ALK5	ALK4
ALK1	C2H6
ALK2	C3H8
HCHO	CH2O
MEK	MEK
OLE1+OLE2	PRPE

Table 3. Mapping table from SAPRC-99 species to MOZART-4 Species.

SAPRC-99	MOZART-4
ALK3[a]+ALK4+ALK5	BIGALK
OLE2	BIGENE
ARO1+ARO2	TOLUENE
OLE1	C3H6
ALK2	C3H8
ALK1	C2H6
ETHE	C2H4
MEK+PRD2	MEK
HCHO	CH2O
CCHO	CH3CHO
ACET	CH3COCH3
MEOH	CH3OH
Not available	C2H5OH[b]

[a] Ethyl alcohol is removed from ALK3 when mapping to BIGALK.

[b] Taken from ethyl alcohol emissions.

Table 4. Spatial proxies used in this work.

Source category	Spatial proxies
Large power plants (>300MW)	Location
Small power plants (<300MW)	Total population
Industry combustion	Urban population
Residential boilers	Urban population
Residential biofuel	Rural population
On-road transportation	Road network
Off-road transportation	Rural population
All other sources	Total population
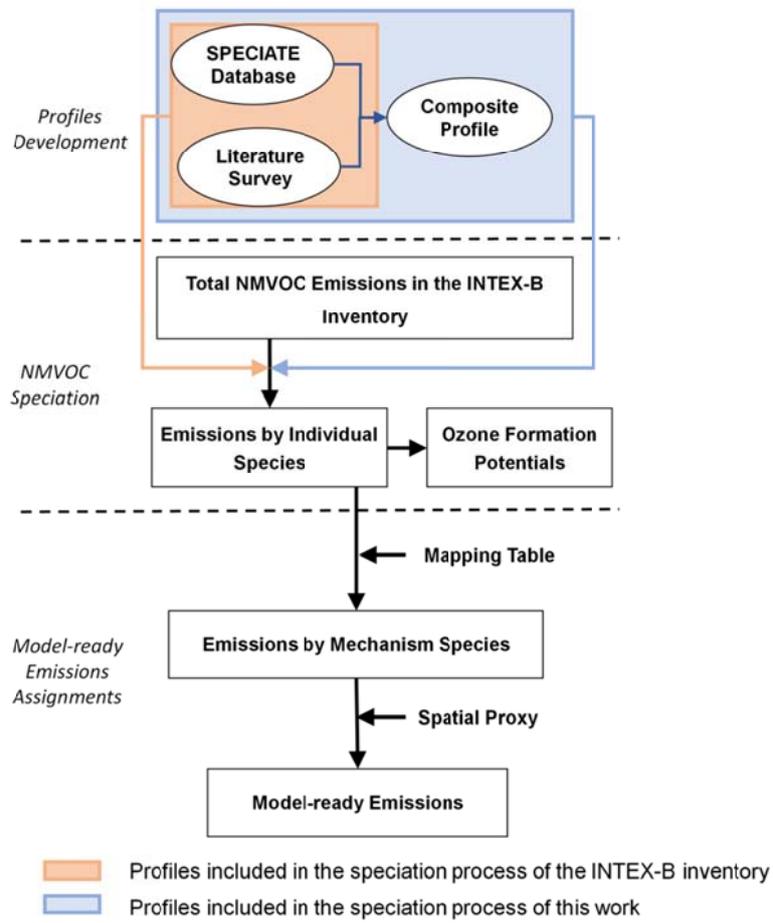
Fig. 1. Schematic methodology of this study.
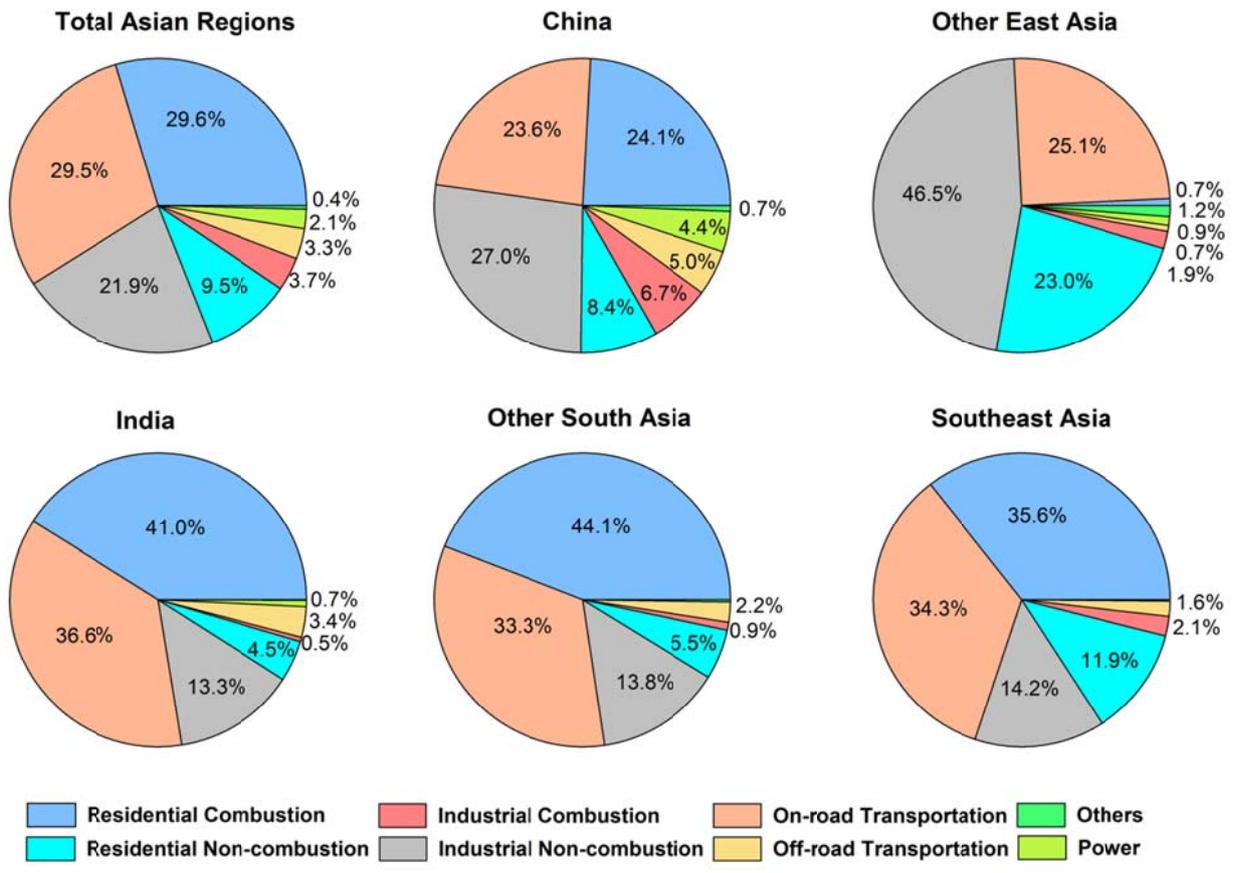
Fig. 2. 2006 NMVOC emissions by Asian regions in the INTEX-B inventory.
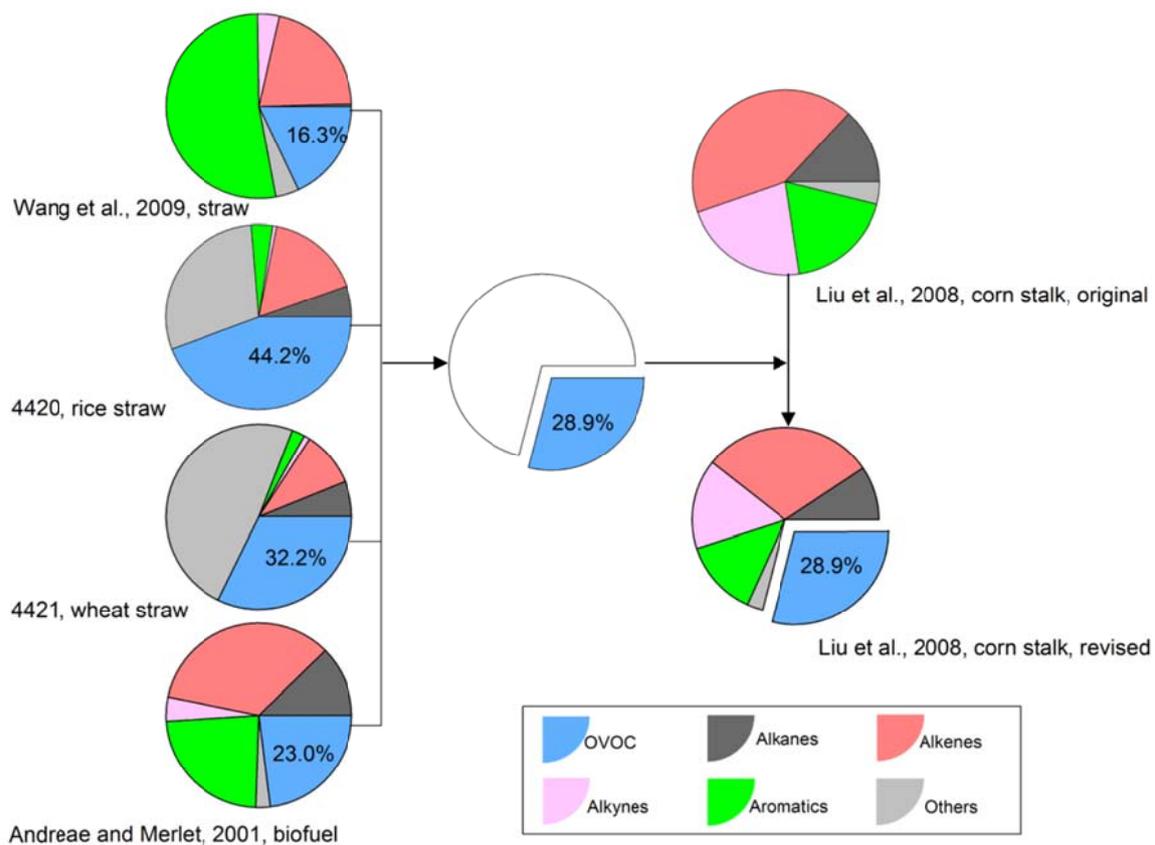
Fig. 3. Inclusion of OVOC fraction for incomplete crop residue combustion profiles. 4420 and 4421 are the "P_NUMBER"s of profiles taken from the SPECIATE database developed by the US EPA.
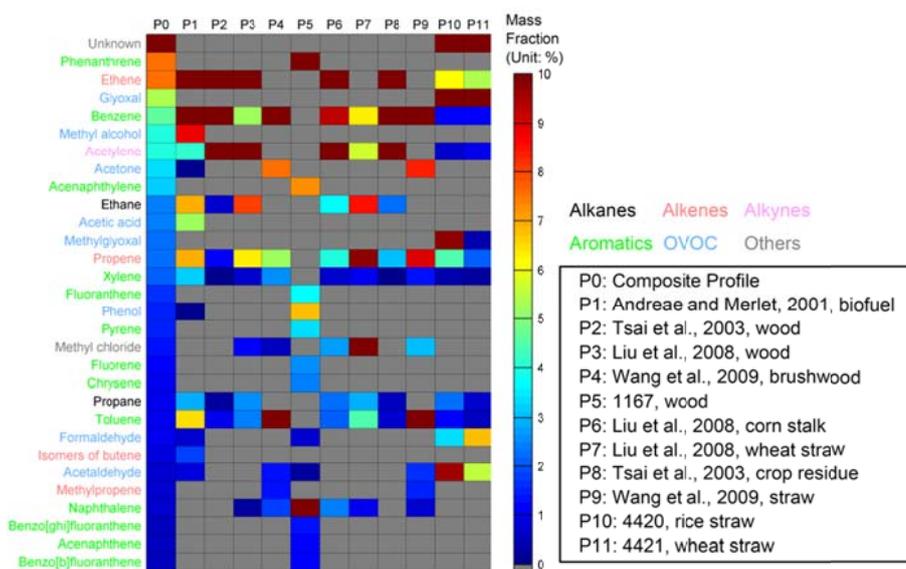
Fig. 4. Mass fraction of major species in the profiles for the residential biofuel combustion. Top 30 species are presented and ranked decreasingly based on the mass fraction in the composite profile (P0). Grey grids indicate that mass fractions for these species are not included in the profile.
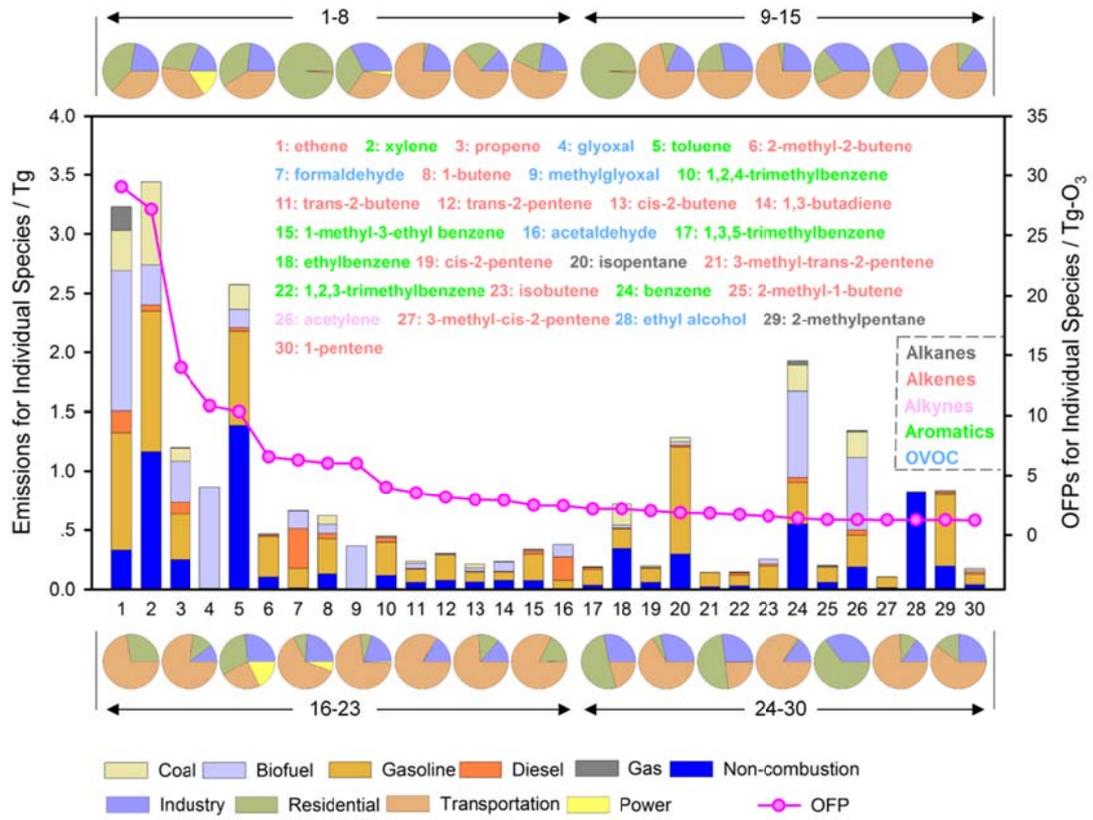
Fig. 5. Emissions by individual NMVOC species and corresponding OFPs.
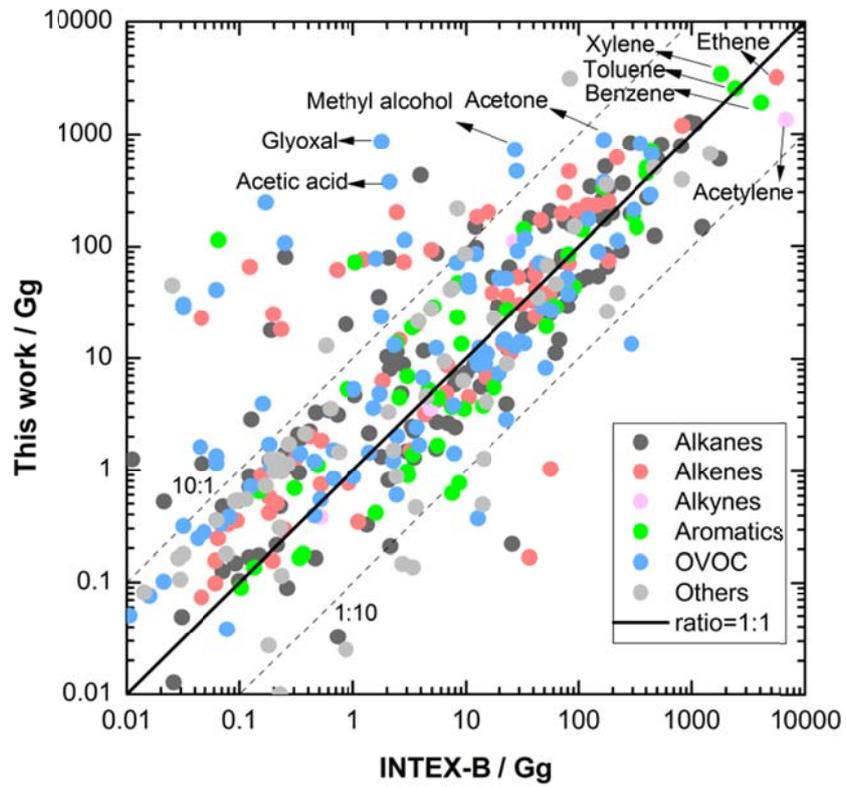
Fig. 6. Comparison of this work and the INTEX-B inventory by individual species.
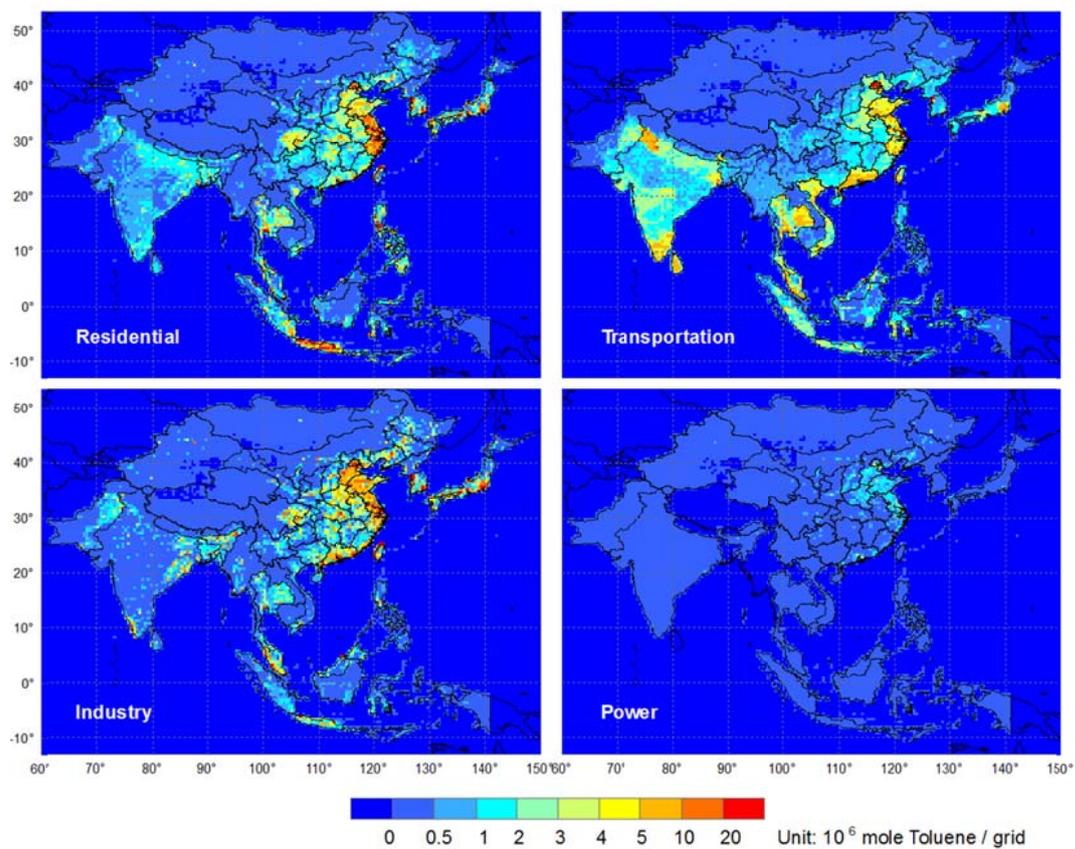
Fig. 7. Emission distribution of toluene by sector at 30 min × 30 min resolution (unit: 10^6 mole yr^{-1} per grid).
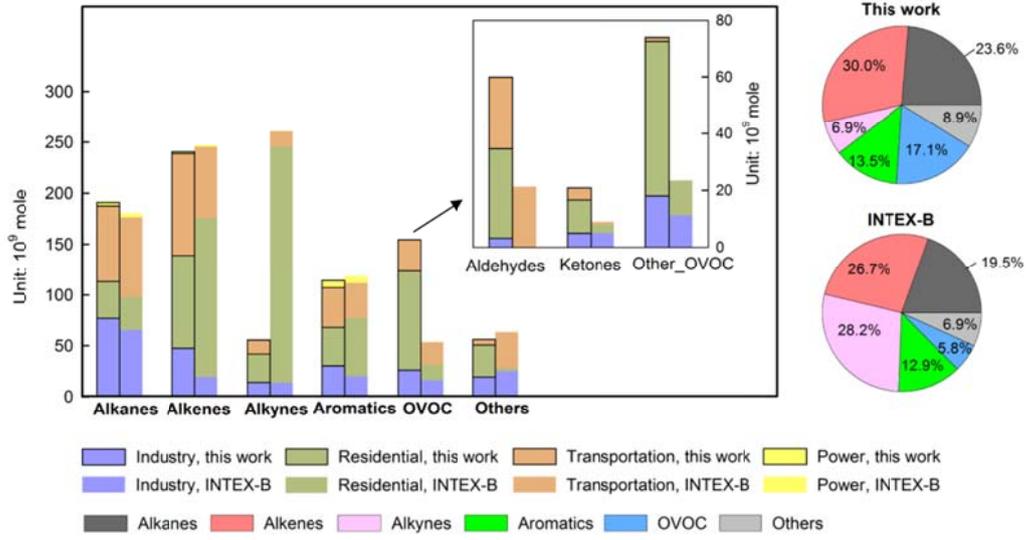
Fig. 8. Asian anthropogenic NMVOC emissions in 2006 by chemical groups.
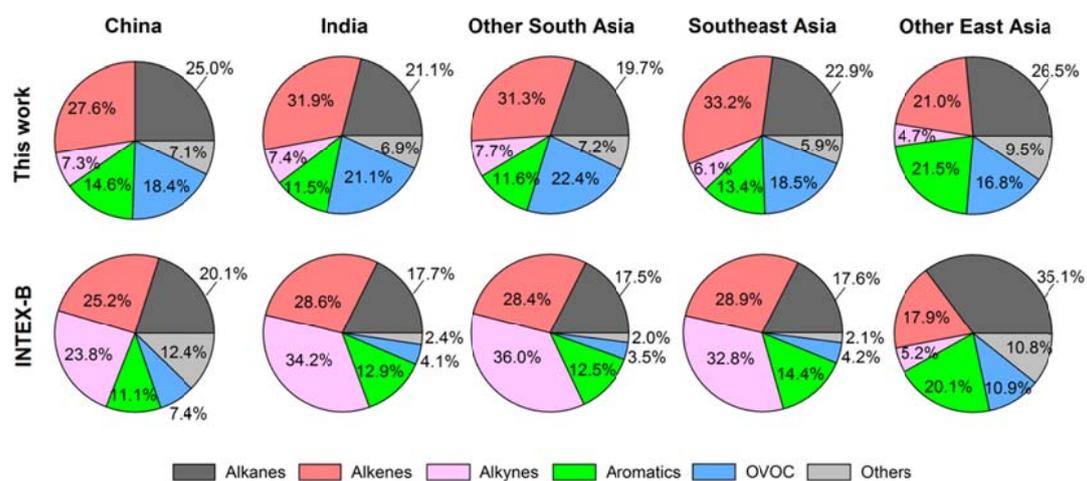
Fig. 9. Distribution of anthropogenic NMVOC emissions in 2006 among different chemical groups for Asia regions.
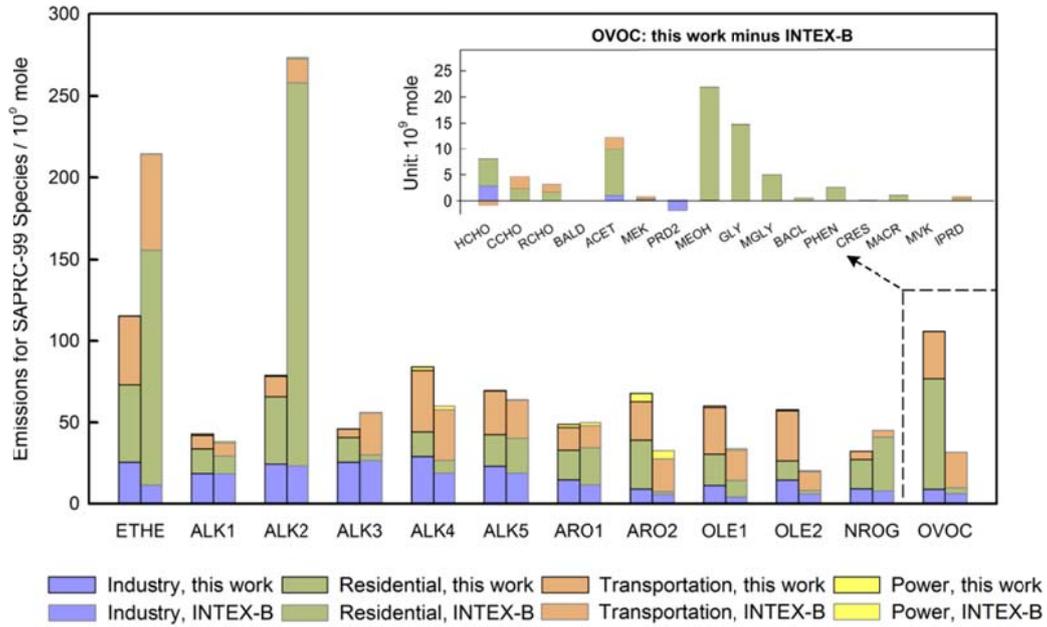
(a) SAPRC-99
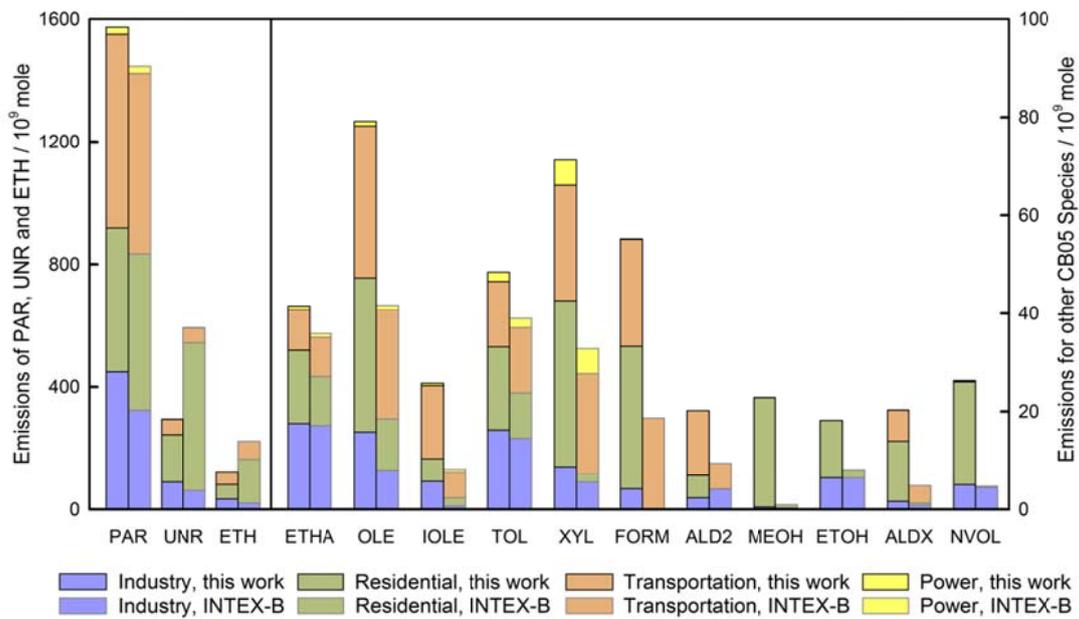
(b) CB05

Fig. 10. 2006 Asian anthropogenic NMVOC emissions by SAPRC-99 (a) and CB05 (b) species. An explanation of the abbreviations of SAPRC-99 and CB05 emitting species are presented in Tables A1 and A2.
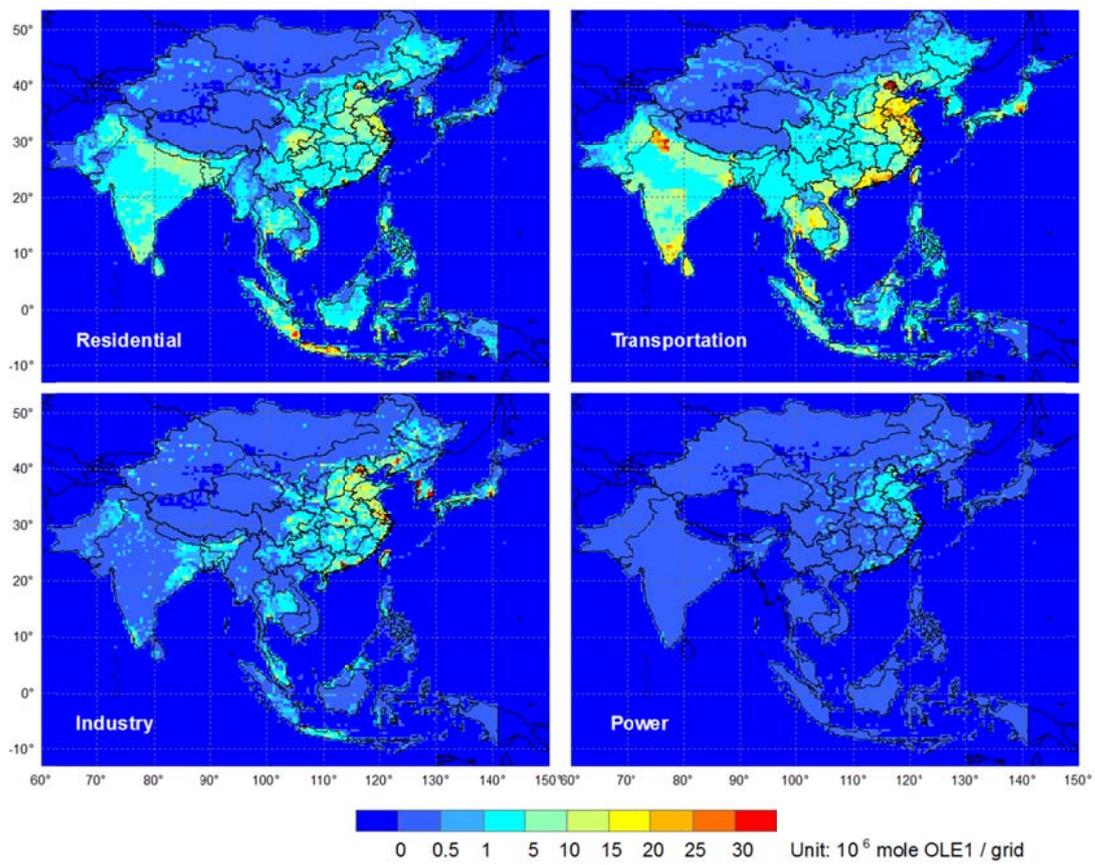
Fig. 11. Emission distribution at 30 min × 30 min resolution of OLE1, SAPRC-99 species.

Fig. 12. 2006 Asian emissions for SAPRC-99 mechanism species by regions.
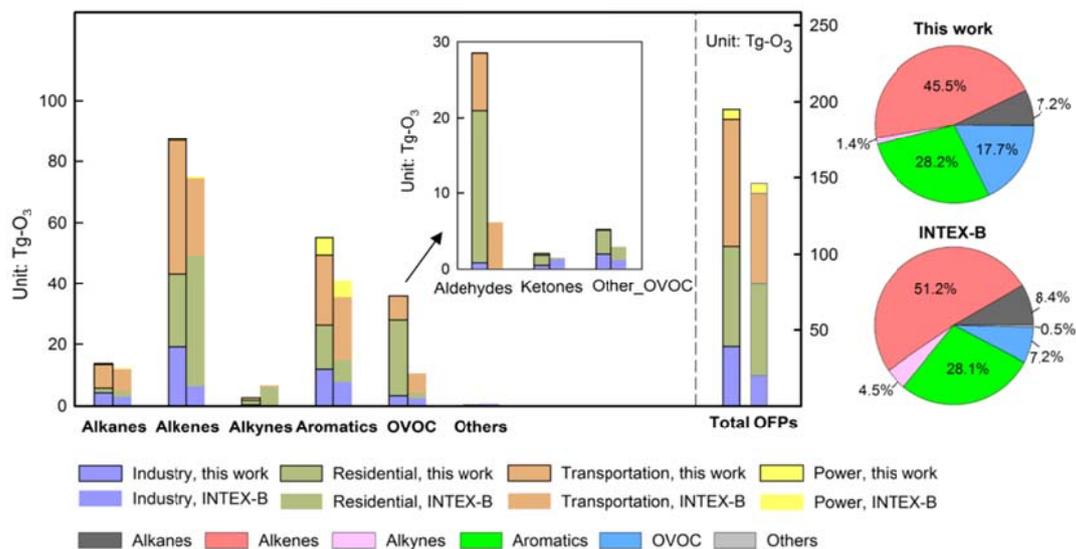
Fig. 13. Ozone Formation Potentials (OFP) of Asian anthropogenic NMVOC emissions in 2006 by chemical groups.
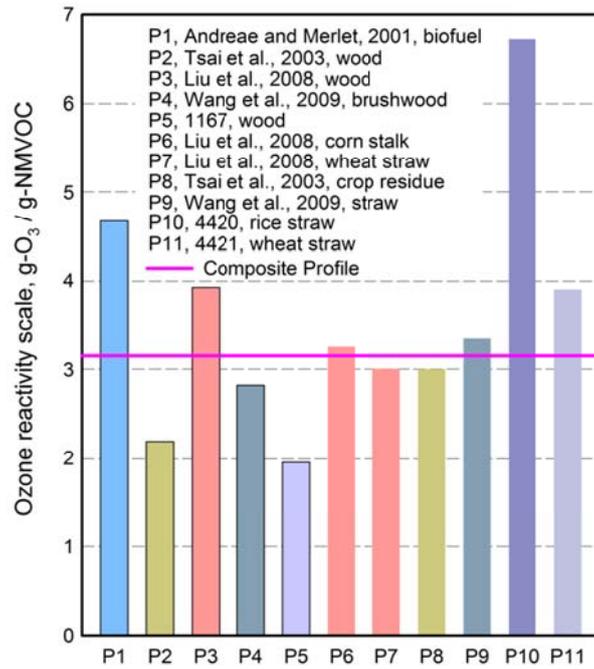
Fig. 14. Sensitivity of OFPs to profile selection for the residential biofuel combustion.
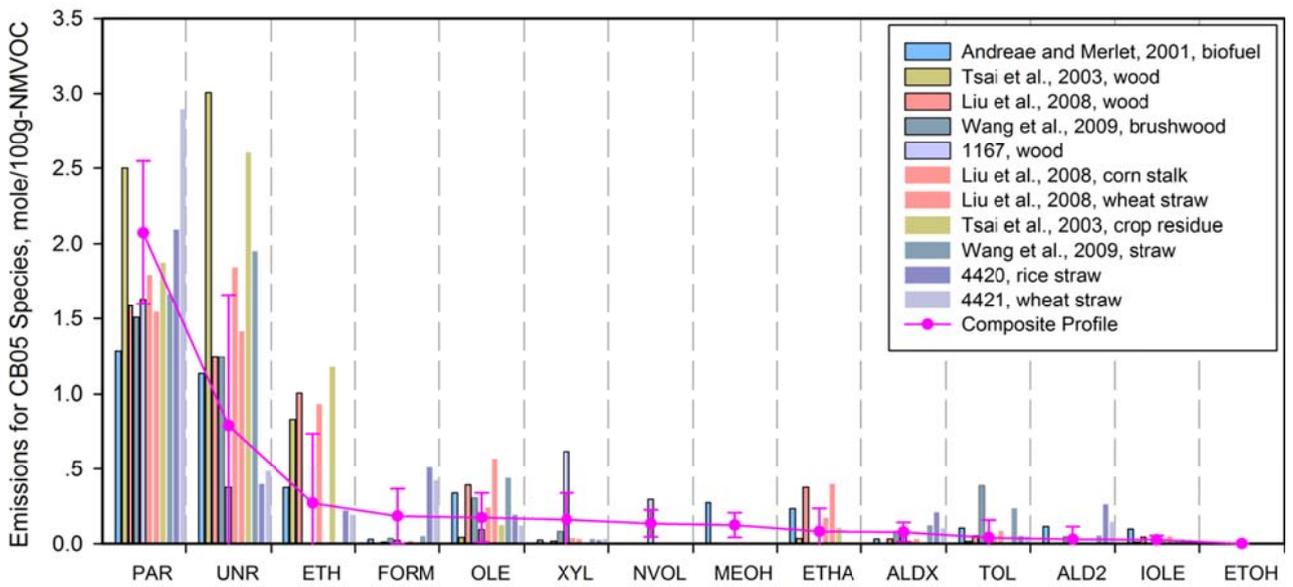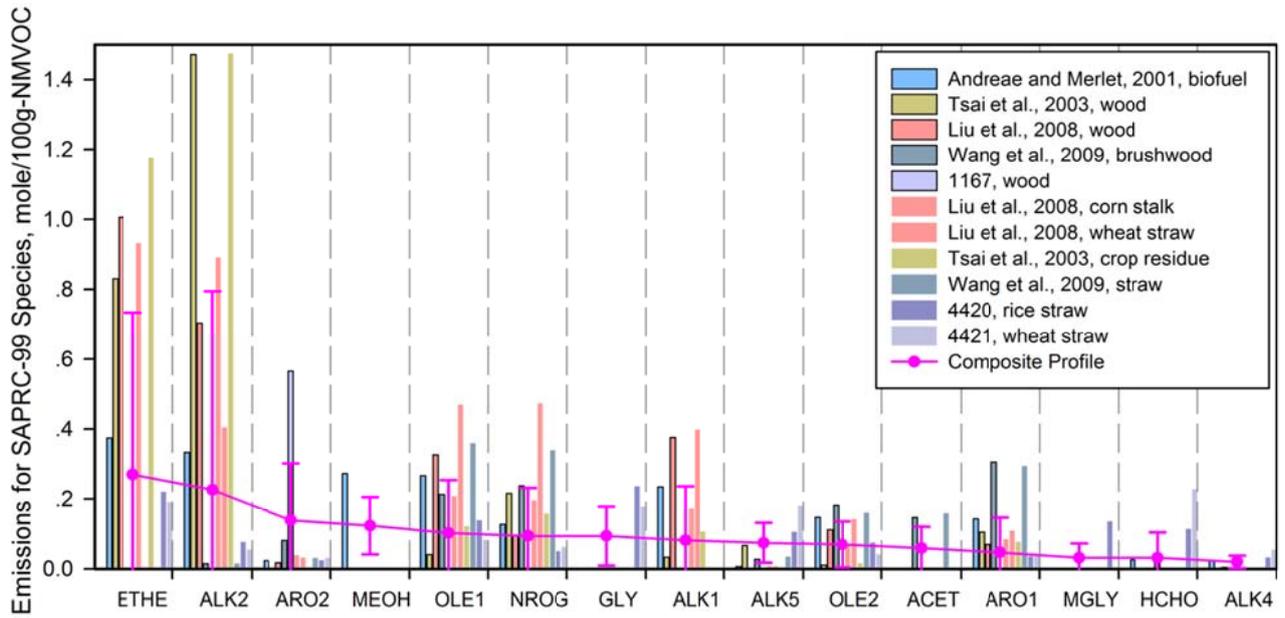
Fig. 15. Sensitivity of model-ready emissions to profile selection for the residential biofuel combustion.